Doctorate Dissertation (Censored)

博士論文（要約）

Analysis of gene expression dynamics in circadian clock synchronization and Akt signaling pathway by optical perturbation systems

（概日時計同調機構と Akt シグナル伝達経路における
光摂動系を用いた遺伝子発現動態解析）

A Dissertation Submitted for Degree of
Doctor of Philosophy
December 2017

平成 29 年 12 月　博士（理学）申請

Department of Chemistry, Graduate School of Science,
The University of Tokyo

東京大学大学院理学系研究科
化学専攻

Genki Kawamura

河村　玄気

Acknowledgments

The present thesis was completed under the supervision of Dr. Takeaki Ozawa, Department of Chemistry, School of Science, The University of Tokyo. I would like to appreciate throughout the research on his support and advice.

I would like to thank all committee members, Dr. Mitsuhiko Shionoya, Dr. Moritoshi Sato, Dr. Koji Harano, and Dr. Yuki Goto for reviewing this thesis with insights and patience.

I would also like to express my gratitude to Dr. Teruya Tamaru in Toho University and Dr. Mitsuru Hattori in Osaka University for their valuable discussions and instructions for the experiments, especially for the topic on circadian clocks.

I would also like to appreciate Dr. Paolo Sassone-Corsi in the University of California Irvine, Dr. Ivor Benjamin in the University of Utah, Dr. Teruyo Tsukada in Riken, Dr. Yasuharu Ninomiya in National Institute of Radiological Sciences and Dr. Ken Takamatsu in Toho University for the support of the materials used in this study.

For analysis of integrative multi omics network, kind support from Dr. Shinya Kuroda Laboratory was grateful for me. Without their help, I could not accomplish the analysis of the data. I especially would like to express my sincere gratitude to Dr. Katsuhiro Kunida, Dr. Daisuke Hoshino, Dr. Atsushi Hatano, Dr. Kentaro Kawata, and Dr. Toshiya Kokaji. In addition, I would like to acknowledge Dr. Tomoyoshi Soga in Keio University for metabolomics measurement with CE TOF-MS experiment and Dr. Yutaka Suzuki in The University of Tokyo for transcriptomics measurement of RNA-seq.

I would like to express sincere thanks to all members of the Analytical Chemistry laboratory. I especially want to thank Dr. Yusuke Nasu, Dr. Yoshihiro Katsura, and Dr. Toshimichi Yamada for valuable advice, Mr. Tomoki Nishiguchi for the discussion, Ms. Yuka Takahashi, Mr. Masashi Miyasaki and Ms. Emi Iwado for encouragements and motivation, Dr. Maki Komiya, Ms. Ayari Takamura, Mr. Masatoshi Eguchi, Mr. Hiroaki Toyota, Mr. Akito Shimizu, Ms. Tsubaki Ota, and Ms. Saki Tomizawa for everyday research. Without them, I could not complete the thesis.

Lastly, I would like to thank my family for their support for doctor course studies, especially Ms. Yumi Hisaoka for everything she did for my support.

Abstract

Transcription is a fundamental process in cellular organisms which transmits genetic information from the genome to actual cellular functions. Recent advancement in sequencing technology enabled researchers to investigate whole genome-wide level transcripts by RNA-seq and microarray hybridization techniques. These techniques provide us rich information about the global landscape of transcription architecture. However, interpretation of the result to understand what contributes to the regulation of transcript is limited. One of the issues is that although RNA-seq technology provides information about transcript abundance, it cannot explain a causative relationship why the expression increased or decreased.

Comparison of results under biologically different condition using a perturbation system is one of the strategies to solve this problem. However, conventional perturbation techniques lack either stimulation of the biological system with precise timings or specificity to a target molecule of interest. Here, I utilized optical perturbation system to overcome these issues and aimed to demonstrate optical perturbation system can be utilized to clarify the causative relationships for transcriptional regulation.

In **Chapter 2**, as to show the concept of adopting optical perturbation system to understand transcriptional regulation which temporal aspect is important for the system, I targeted physiological timing system, the circadian clock. Using UV irradiation as an optical perturbation system, I analyzed causative relationships on circadian time-dependent regulation of a clock gene, *Per2*. In this study, I used reporter assay to precisely quantify transcript abundance in real-time. By the combination of optical perturbation and temporal transcript profiling by the reporter assay, circadian time-dependent transcriptional regulation on *Per2* was identified.

In **Chapter 3**, the global assessment of molecules by the omics analysis was used to identify the causative relationships of the transcriptional regulation. Insulin, a hormone that regulates glucose metabolism in the cell is one of the examples of a signaling pathway regulating complex signaling output. Akt is a kinase that is reported to play a central role in the insulin signaling. To dissect the role of Akt in the insulin signaling pathway, I employed optical perturbation system using the optogenetic tool, which enables Akt specific activation upon light illumination. To fully characterize the action of Akt, I compared the effect of Akt specific activation and insulin stimulation. By integrating multi omics information from metabolome to transcriptome, the molecular mechanism of the Akt-dependent signaling was identified.

In this dissertation, I will describe that optical perturbation system can be used to identify the transcriptional regulation mechanism by demonstrating these two studies.

Table of Contents

Abbreviations

3C	Chromosome conformation capture
3T3-L1	3T3-L1 pre-adipocyte cells
ADP	Adenosine diphosphate
AMP	Adenosine monophosphate
ANOVA	Analysis of variance
AS160	Akt substrate of 160 kDa
ATP	Adenosine triphosphate
ATCase	Aspartate transcarbamylase
BMAL1	Brain and Muscle Arnt-like 1
BRENDA	Braunschweig Enzyme Database
BS	Bovine serum
C2C12	C2C12 myoblast cells
cDNA	Complementary DNA
CDP	Cytosine diphosphate
C/EBPα	CCAAT-enhancer-binding protein alpha
CE TOF-MS	Capillary electrophoresis time-of-flight mass spectrometry
ChIP	Chromatin immune-precipitation
Cibn	Cryptochrome interacting basic-helix-loop-helix n-terminus
CLOCK	Circadian Locomoter Output Cycles Kaput
CMP	Cytosine monophosphate
CPSase	Carbamoyl-phosphate synthase
CRISPR	Clustered regularly interspaced short palindromic repeats
Cry	Cryptochrome
CSA	10-camphorsulfonic acid
CT	Circadian time
CTP	Cytosine triphosphate
Dex	Dexamethasone
DHAP	Dihydroxyacetone phosphate
DHOase	Dihydroorotase
DMEM	Dulbeco's Modified Eagle Medium
DNA	Deoxyribonucleic acid
DTT	Dithiothreitol
E-Box	Enhancer box
ECFP	Enhanced cyan fluorescent protein
EDTA	Ethylene diamine tetra-acetic acid
EGFR	Epidermal growth factor receptor
F1,6P	Fluctose-1-6-biphosphate
F6P	Fluctose-6-phosphate
FAD	Flavin adenine dinucleotide
FBS	Fetal bovine serum
FDR	False discovery rate
FoxO1	Forkhead box protein O1
FPKM	Fragments per kilobase million

G6P	Glucose-6-phosphate
GDP	Guanine diphosphate
GEO	Gene Expression Omnibus
Glut4	Glucose transporter type 4
GMP	Guanine monophosphate
Gsk	Glycogen synthase kinase
GTP	Guanine triphosphate
Hk	Hexokinase
HS	Heat-shock
HSE	heat-shock element
HSF1	Heat-shock factor 1
Hsp40	Heat-shock protein 40 kDa
Hsp70	Heat-shock protein 70 kDa
Hsp90	Heat-shock protein 90 kDa
HSR	Heat-shock response
IBMX	3-isobutyl-1-methylxanthine
IgG	Immunoglobulin G
IP	Immuno-precipitation
iPS	Induced pluripotent stem
IRS	Insulin receptor substrate
KEGG	Kyoto Encyclopedia of Genes and Genomes
*Mdm*2	Mouse double minute 2 homolog
MEFs	Mouse embryonic fibroblasts
MES	2-[N-morpholino] ethanesulphonic acid
mRNA	messenger ribonucleic acid
MTHFD2	Methylenetetrahydrofolate dehydrogenase/cyclohydrolase, mitochondrial
mTOR	mammalian target of rapamycin
myr	myristoyl sequence
NaN	Not a number
NCBI	National Center for Biotechnology Information
NIH3T3	National institute of health 3T3 cells
NP-40	nonyl phenoxypolyethoxylethanol
n.s.	not significant
p53RE	p53 response element
p70S6K	Ribosomal protein S6 kinase beta-1
P/S	Penicillin and streptomycin
PA-Akt	Photo-activatable Akt
PAGE	Polyacrylamide gel electrophoresis
PBS	Phosphate buffered saline
PCR	Polymerase chain reaction
PDK1	Phosphoinositide-dependent kinase-1
*Per*2	*Period*2
PH	Pleckstrin homology
PI3K	Phosphoinositide 3-kinase
PKA	Protein kinase A
PKC	Protein kinase C

PPARγ	Peroxisome proliferator-activated receptor gamma
PRC	Phase response curve
PTC	Phase transition curve
qPCR	quantitative polymerase chain reaction
RIPA	Radio immunoprecipitation assay
RLU	Relative Luminescence Units
RMA	Robust Multiarray Average
RNA	Ribonucleic acid
RNA-seq	RNA sequencing
ROS	Reactive oxygen species
SD	Standard deviation
SDS	Sodium dodecyl sulfate
SLR	Stable Luciferase Red
smFISH	single-molecule fluorescent *in situ* hybridization
SOS	Son of sevenless
SREBP	Sterol regulatory element-binding protein
TCA cycle	Tricarboxylic acid cycle
UDP	Uridine diphosphate
UMP	Uridine monophosphate
UTP	Uridine triphosphate
UV	Ultra violet

Chapter 1

General Introduction

1-1. Transcriptional regulation in cellular systems

Genetic information that each cell poses is expressed as a cellular function by transcription of the genome to RNA.[1,2] Regulation of gene expression is tightly determined in cell type-specific and/or environmental context manner, making transcription as an important feature in the understanding of determination of a cell state.[3] Recent studies show the diverse mechanism of controlling the abundance of transcripts, including activation of transcription factors to enhance gene expression, miRNA or RNA binding protein-induced regulation of transcripts lifetime.[4–6] Because these mechanisms often function in a cooperative manner, identification of causative relationships toward regulation of transcription is difficult (**Figure 1-1**).[7,8]

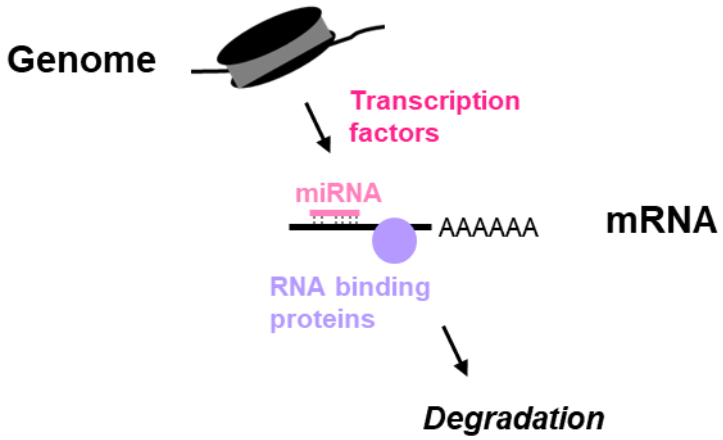

Figure 1-1. Transcriptional regulation in mammalian cell.
Transcriptional regulation is controlled with multiple modes. The abundance of the transcript is determined by transcription from the genome and degradation of the transcript. Transcription factors enhance transcription to increase transcript abundance. RNA binding proteins and miRNA binds to a transcript and modulates its lifetime. Combination of these regulation modes occurs for each transcript.

Since transcripts account for regulation of translated protein abundance, and single transcript can be used as a template for translation for multiple times, transcriptional regulation is especially influential to a cellular system with a long-time scale (i.e. hours, days). Examples include cellular differentiation, a phenomenon that transforms cellular character during development. For instance, in cellular reprogramming to induced pluripotent stem cell (iPS cell), four transcription factors are introduced to cells to induce the phenomenon.[9] Also, cellular differentiation is associated with induced expression of specific transcription factors; muscle differentiation for MyoD,[10] adipocyte differentiation for Peroxisome proliferator-activated receptor gamma (PPARγ) and CCAAT-enhancer-binding protein alpha (C/EBPα).[11] Additionally, a timing system of living organisms,

the circadian clock is regulated by transcription of clock genes, which is tightly regulated by transcription and post-transcriptional regulation mechanisms.[12] Thus, transcriptional is closely associated with the fundamental process of cellular organisms, and its regulation is tightly regulated for the specific biological phenomenon.

In order to understand causative relationships of transcript regulation, both a quantification method of the transcript and an experimental framework for identification of the causative regulation are necessary.

1-2. Conventional methods to analyze the quantity of a transcript

Because of the fundamental importance of transcriptional regulation to cellular systems, biological techniques to analyze the quantity of transcripts in a cell are intensively developed. These methods are classified into two, the one which focuses on the specific transcript and the other which globally analyze transcripts in an unbiased manner (**Figure 1-2**). The targeted approach has the advantage of high sensitivity to the target, making it an ideal tool to analyze the abundance if the target is selected. The unbiased approach has the advantage of objectiveness, which has the potential to detect conventionally unknown targets. However, unbiased approach is weak in sensitivity. Because these methods are complementary to each other, a combination of these two approaches is able to cover the weakness of each approach.

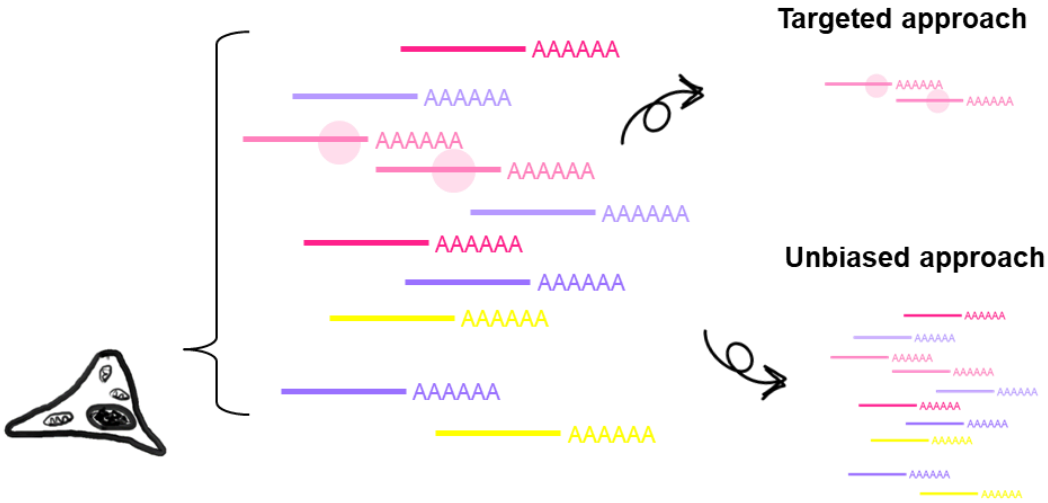

Figure 1-2. Two approaches for the analysis of transcriptional regulation.
Cells comprise numerous number and types of transcripts. The targeted approach focuses on the specific transcript and extracts information about the target transcript. The unbiased approach aims to measure all transcripts that exist in the sample.

The targeted method includes both biochemical and genetic techniques. Most commonly used biochemical methods are northern blotting[13] and quantitative polymerase chain reaction (qPCR). More recently, digital PCR method is developed for precise quantification of the transcript based on separation of PCR reaction mixture by microfluidics to accurately measure the result of PCR reaction.[14] Basic strategy that biochemical methods have in common is the use of complementary DNA (cDNA) for the detection of the target transcript. Northern blot hybridizes detectable cDNA to reverse transcribed RNA after electrophoresis separation for the detection. Quantitative PCR and digital PCR methods amplify target transcript by PCR reaction using complementary sequence against the target gene.[15] Because these methods use cDNA that has high selectivity to the target transcript, highly selective detection of the transcript is accomplished. In addition, owing to the amplification character of the PCR protocol, a highly sensitive detection is achieved for methods with the PCR process.

A representative genetic method is reporter assay (**Figure 1-3A**). A reporter assay is one of the powerful techniques to enable an optical visualization of gene expression or a protein localization.[16] In reporter gene assay, promoter of the gene of interest is fused to a gene of the optically visible probe (i.e. a bioluminescent protein, a fluorescent protein). By doing so, optically visible probes are expressed as in the same manner as transcriptional regulation of a gene of interest. Because probe's signal can be optically detected, regulation on a gene of interest can be visualized by the signal from the probe. Among reporter genes, bioluminescence emitting enzyme, a luciferase, is especially a powerful tool in observation of gene expression by its character of emitting luminescence without an external light source (**Figure 1-3B**).[17] The absence of an external light source for the observation enables detection of gene expression without perturbation of the cellular system during the assay. Furthermore, because it only requires a photon detector for the detection of the bioluminescent signal, a bioluminescence assay could be operated in a high throughput manner. Up to date, several types of luciferase is used in a reporter assay, including luciferase from firefly (*Photinus pyralis*),[18] railroad worm (*Phrixothrix hirtus*), sea pansy (*Renilla reniformis*)[19] and deep-sea shrimp (*Oplophorus gracilirostris*).[20] A beetle luciferase, firefly luciferase, and railroad worm luciferase emits green to red color in the spectrum and uses the same type of substrate, D-luciferin. On the other hand, marine luciferase, *Renilla* luciferase, and deep-sea shrimp luciferase emits bioluminescence at the blue-green color on the spectrum and uses derivatives of coelenterazine as a substrate. Although luciferases from a marine organism have a tendency to emit brighter luminescence than the beetle luciferases, they lack the ability for long-term observation due to the rapid decay of the signal caused by instability of its substrate. Because observation of transcript expression profile requires temporally stable expression, characteristics of beetle luciferases that utilize more stable D-luciferin as a substrate is most suited for analysis of transcription architecture.

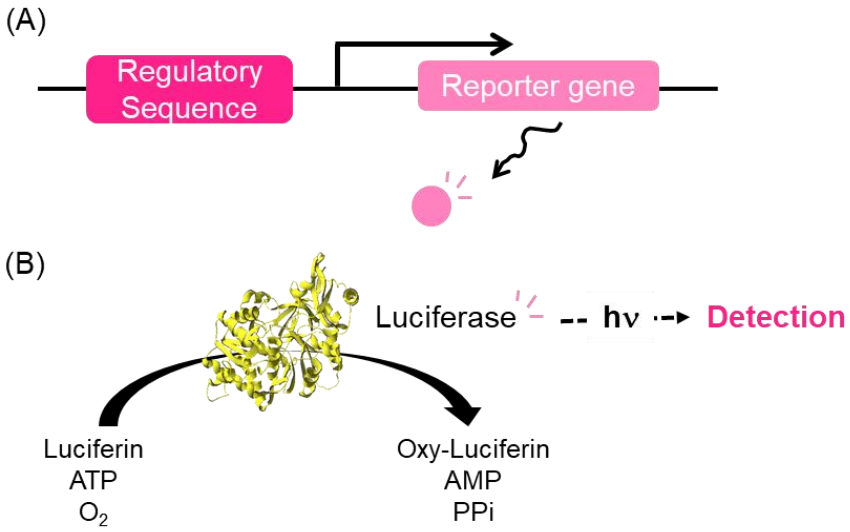

Figure 1-3. Reporter gene assay by bioluminescent protein, luciferase.
(A) Schematics of the reporter gene assay. When reporter gene is fused to a regulatory sequence or promoter of a gene of interest, the reporter gene is expressed in the same manner as transcriptional regulation on that sequence. (B) Enzymatic reaction of a luciferase. Luciferase catalyzes a reaction that converts luciferin to oxy-luciferin. During the process, light is generated. By detecting this signal, the amount of luciferase can be quantified.

In contrast to targeted methods, unbiased methods enable a global analysis of gene expression, leading to quantification of the expression of the gene of interest.[21] The unbiased method includes microarray hybridization and RNA sequencing (RNA-seq). In microarray analysis, an array of synthetic DNA in microwell plate allows detection of a set of the transcript at once.[22] In a microarray experiment, fluorescently labeled sample DNA which is reverse transcribed from transcripts are hybridized to the fixed cDNA probes in a well plate format. By measuring the fluorescent intensity in each well, amount of transcript that exists in the sample can be quantified (**Figure 1-4**). Although microarray experiment provides the global expression profile of the transcript, coverage of transcript is limited to the selection of a cDNA probe set. This can be both pros and cons since the limitation of fixed cDNA probe sets enables highly sensitive detection of a probe set of interest (i.e. kinases only). However, if one wishes to perform genome-wide unbiased expression profiling, many cDNA probe sets are to be used, which makes the experimental design complex.

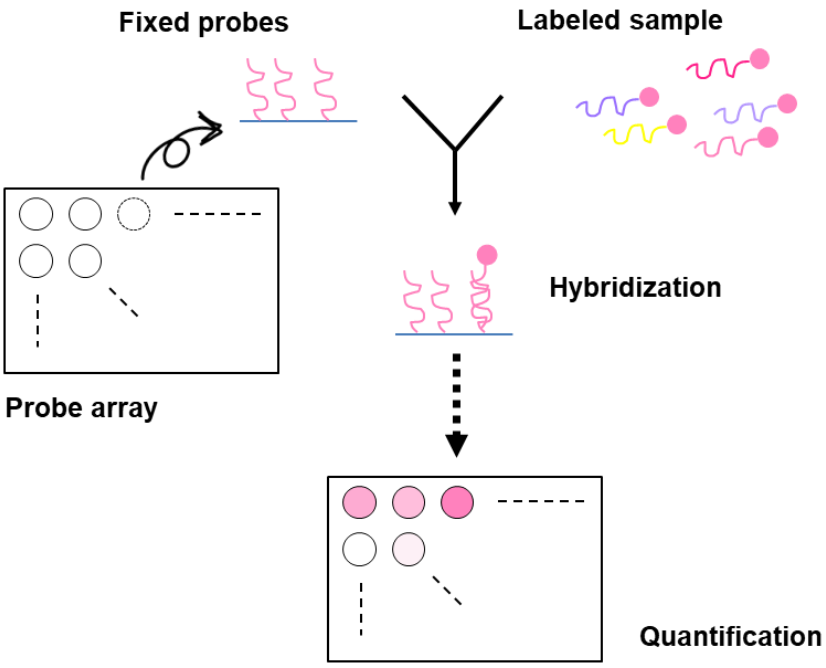

Figure 1-4. Schematics of microarray hybridization.
cDNA probe sets are arrayed to a welled-plate. Transcripts contained in the sample are reverse transcribed and labeled with fluorescent dye. Labeled samples are applied to each well, and if the sample contains transcripts with a complementary sequence to the fixed DNA probe, then hybridization occurs. By measuring the intensity of the labeled fluorescent dye of a sample, the amount of transcript can be estimated.

More recently, the RNA-seq method that quantifies transcripts at a whole genome-wide level has drawn much attention owing to unbiased and rich information about transcripts it provides (**Figure 1-5**).[23] In contrast to microarrays, RNA-seq literally reads sequences of transcripts from the sample. Because of this character, RNA-seq has the potential to detect isoform specificity, splicing junctions and also an ability to identify novel transcripts.[24,25] Because RNA-seq analysis maps read sequences to the genomic sequence, transcripts with longer length has a tendency to get the large number for the quantity. In order to normalize transcript abundance according to the transcript length, a value such as fragments per kilobase million (FPKM) is used. FPKM value corresponds to the number of reading sequence mapped to the transcript, normalized to the transcript length by a kilobase, and further normalized to a fraction in million reads for further comparison between data. Although several normalization protocols exist, abundance detected by RNA-seq is comparable between analyzed transcripts. Thus, RNA-seq has the potential for relative quantification of all transcripts exists in the sample. For the sensitivity of the method, the number of sequencing reads determine the detection limit of low abundant transcripts. Accordingly, setting the optimal RNA-seq protocol is a key issue in the coverage of the transcript to be analyzed.

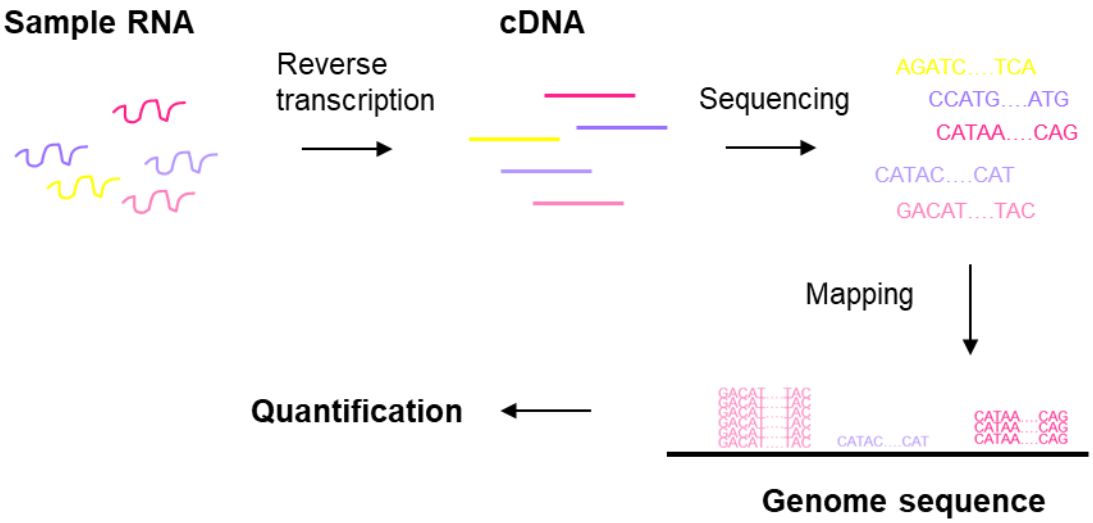

Figure 1-5. Schematics of RNA-seq experiment.
RNA extracted from the sample are reverse transcribed to cDNA. Massively parallel sequencing of transcribed cDNA (million to billion) are performed. Read sequences are aligned to the genomic sequence originated from the sample. By quantifying the number of mapped sequences on the transcript, an abundance of the transcript is analyzed.

1-3. Conventional perturbation methods for transcriptional regulation analysis

Above mentioned methods allow researchers to analyze transcripts quantity in a cellular system either globally or locally. However, a discovery of cellular transcriptional regulation requires identification of its causative relationships. In order to reveal the causative regulation of a transcript, estimation of molecules that are responsible for the regulation is necessary. For this aim, a change in transcript abundance after perturbation of the biological system provides the key for identifying the essential component of the regulatory machinery. Because transcriptional regulation is associated with the transcription and a transcript lifetime, analysis of transcript abundance, in turn, provides an insight into the regulation mode. For instance, if the transcript abundance increased, transcriptional activation or a prolonged lifetime of the transcript is inferred. By linking the biological event that the perturbation induces with the inferred transcriptional regulation modes, molecules that are responsible for the regulation can be estimated. Thus, selection of the perturbation system is important for revealing the transcriptional regulation.

Conventionally, genetic or chemical perturbation are widely used. Genetic perturbation, for instance, nucleotide variants in the genomic DNA, perturbs cellular system persistently. The advantage of the genetic perturbation is that the cause of transcriptional regulation difference can easily be associated with the genetic variant. However, analysis by genetic perturbation has the

following disadvantages. One is that it is difficult to introduce a genetic variant to the cellular genome. Typically, introducing a genetic variant takes about a month, and during the process, cellular adaptation might occur to compensate the perturbation. The other disadvantage is that a genetic perturbation is typically a binary perturbation, that is whether the system is perturbed or not, which will hamper analysis of intermediate events. In contrast, chemical perturbation systems apply activator or a repressor of a signaling molecule to investigate the role of the target molecule. Because chemicals can be delivered in a high temporal resolution manner, undesired signaling adaptation can be avoided. Also, since chemicals can be administrated in a dose-dependent manner, the detailed perturbation can be achieved. However, target molecule limitation exists for a chemical perturbation, because activators or inhibitors for not all the molecules are developed. Also, specificity of the chemical for the target molecule is another concern when using chemical perturbation. As an example, the phosphoinositide 3-kinase (PI3K) inhibitor wortmannin also blocks mammalian target of rapamycin (mTOR) and other kinases as well, since catalytic domains of these proteins are similar. Thus, perturbation system that can precisely activate or inhibit the target molecule in both high temporal and dose-dependent manner is required for the transcriptional regulation research.

Recently, light-dependent actuators from optogenetic technique were developed as a perturbation system of the cellular signaling pathway. An advantage of optical perturbation system lies in its precise tuning of perturbation stimulation in both space and time with dose dependency. Additionally, when an optogenetic probe is used, an optical perturbation system also allows selective activation of the target molecule. These characters of optical perturbation system provide an additional option for the selection of the perturbation system for investigating the causative relationships of transcriptional regulation.

1-4. Comparison of the time resolution of perturbation methods

For the analysis of transcriptional regulation, time-resolution of the perturbation is especially important, because transcriptional regulation upon stimulation is usually a transient phenomenon. For instance, the transcriptional regulation is associated with cellular adaptation, a system to adjust cellular environment to the perturbed state. Thus, in this section, I will compare the time resolution of each perturbation system. Especially, the on-time and the off-time time resolution of the perturbation system is considered, because the on-time and the off-time time resolution differs greatly among systems.

The time resolution of the perturbation system differs by the type of stimulation (**Table 1-1**). For example, because genetic perturbation like gene knock-out or gene knock-in methods modifies genome for the perturbation, on time of the perturbation depends on the time when cells after genetic modifications were established. However, the off time is practically infinite since genomic

modifications are persistent for the cell. RNA interference and overexpression of the target gene are methods that transiently decrease or increase transcripts abundance without modification of the genome.[26,27] The on-time and the off-time time resolution for these methods depends on the transduction of the probe nucleotides to the cell. Expression of the probe takes hours to days, depending on the cellular condition. Thus, although genetic perturbation methods have high specificity for the target, the time resolution for the genetic perturbation methods is low.

For chemical stimulation, the action of chemicals is fast, enabling rapid perturbation of the system. On the other hand, the off time of the stimulation cannot be controlled, since administrated chemicals cannot be removed unless the chemicals are washed out. Recently, microfluidics techniques that enable flow type stimulation were developed which enables temporal control of administration pattern of the perturbation.[28] Methods that combine microfluidics have high time resolution for both the on time and the off time of the stimulation. However, at present, microfluidics device is difficult to be integrated for the detection systems, limiting its applications for the analysis of the cellular phenomenon. Taken together, chemicals have a high temporal resolution for the on time of the perturbation, but it requires additional devices for shortening the off-time time resolution.

Light stimulation has a great advantage over these techniques for the off-time time resolution of the perturbation. Because in optical perturbation systems, the on time and the off time of the perturbation corresponds to the time illuminated, no other process is necessary to terminate the perturbation. Owing to high temporal resolution for the switching of the perturbation, temporally precise stimulation is enabled by the optical perturbation system. However, conventional light stimulation such as UV irradiation or γ-ray irradiation has low specificity for perturbing the target molecule. To overcome this issue, optogenetic techniques that allow target-specific control by light illumination are developed.[29,30] Optogenetics utilize fusion protein of photoreceptors and target proteins or domains. Optogenetics has high temporal control owing to the property of light for the activation of the system and an ability to activate a specific target. These advantages make optogenetic techniques an ideal tool for analyzing the effect of the target molecule with perturbation at a desired timing.

Another type of perturbation is achieved by using either a chemogenetics tools[31,32] or a thermogenetics tools.[33,34] Similar to optogenetics tool, these "-genetics" tools utilize chemical- or heat-sensing protein or domains to control the function of specific molecules by administration of a chemical or applying heat. Since chemogenetics utilize a chemical for the perturbation, chemogenetics still has a disadvantage in the off-time time resolution for the stimulation. Recently developed thermogenetics tool utilize an infrared laser for the heating predefined region of interest for the perturbation. Because thermogenetics also use light for the stimulation, thermogenetics also has an advantage of optical perturbation in principle.[33] However, because the off time of the perturbation depends on the cooling time of the heated system, the off-time time resolution of the thermogenetics is considered to be low comparing to optical perturbation systems. Although improvements of these

techniques may overcome these limitations, currently, optical perturbation system including optogenetics an optimal tool for perturbing the biological system with a high temporal resolution.

Type of perturbation		Time resolution (ON)	Time resolution (OFF)	Spatial resolution	Specificity
Genetic	Knock-out, Knock-in	-	-	-	Target specific
	RNAi, Over expression	h-day	-*1	-	Target specific
Chemical	Activators, inhibitors	ms – min	-*2	-	Relatively high *5
	Combined with microfluidics	ms – min	sec - min	-	Relatively high *5
	Chemogenetics	ms – min	-*2	-	Target specific
Light	UV, gamma-ray	ms – min	sec - min	μm- *4	Low
	Optogenetics	ms – min	sec - min	μm	Target specific
Heat	Thermogenetics	sec – min	min - h*3	μm	Target specific

Table 1-1. Comparison of perturbation methods

*1: Turned OFF when the expression of a perturbation probe is lost (h - day).
*2: Could be turned OFF if administrated chemicals were washed out.
*3: OFF time depends on the cooling time of the perturbed system.
*4: Spatial resolution depends on the wavelength and equipment for the exposure.
*5: Specificity depends on the type of chemical.

1-5. Purpose of the present dissertation

In this thesis, I aimed to prove the concept of combining the optical perturbation system and analysis of transcripts abundance for revealing the causative relationships in biological events. Analysis of cellular transcriptional regulation includes at least two steps. The first step is the identification of candidate signaling molecules that are responsible for the regulation mechanism. The second step is the verification and characterization of the identified mechanism to examine whether the identified molecule is truly responsible for the regulation. In this thesis, I designed an experimental framework that utilizes optical perturbation system for identification of the causative regulation of the transcript involved in the biological events. Among advantages of optical perturbation system, I focused on high temporal resolution of the optical stimulation delivery and selective activation of the target molecule. For the quantification of transcript abundance, I utilized both targeted analysis and unbiased global transcriptome analysis. Because the targeted approach is suited for precise analysis of transcript abundance, a combination of a targeted approach and temporally precise perturbation was applied for the research described in **Chapter 2**. Additionally, a combination of an unbiased approach and selective activation by

optical perturbation is described in **Chapter 3**.

In **Chapter 2**, I selected circadian clock synchronization as a target of the analysis. It is known that the circadian system comprises a transcription-translation feedback loop to maintain its daily oscillation.[35] In this case, the target biological system (the circadian clock) and its component (clock genes) are already identified. Thus, I utilized a targeted approach, a bioluminescent reporter assay, to reveal the molecular mechanism involved in the synchronization of the circadian clock. One of the remaining mysteries in circadian clock synchronization is a circadian time-dependent process involved in the synchronization. Analysis of the molecular mechanism of the circadian time-dependency was conventionally conducted with chemical stimulation using cultured cells because synchronization of the clock rhythms can easily be controlled. Accordingly, I analyzed circadian gene expression in cultured cells using a reporter of the clock gene promoter. Time-resolution for the analysis of time-dependency is limited by activity duration of synchronizing stimulation in the cell, and also by the off-time time resolution of the perturbation. To improve the off-time time resolution of the perturbation, I utilized optical perturbation system using ultra-violet (UV) irradiation. By measuring the transcriptional regulation of the clock gene upon UV irradiation, time-dependent property of the clock system would be identified.

In addition, a system to monitor the activity of the candidate modulator is necessary for deciphering the molecular mechanism of time-dependent regulation on the clock genes. In this chapter, I focused on transcription factors which are known to be activated by the UV stimulation. Hence, I generated reporter assay system for real-time monitoring of the activity of transcription factors activated by UV irradiation. By integrating the optical perturbation system by UV irradiation and analytical system by reporter gene assays, time-specific stimulation and real-time monitoring of the effect of perturbation would be achieved. This integrated system leads to time-dependent activity monitoring of the factors influencing the circadian clock synchronization. Comparison of time-dependent transcriptional regulation of clock gene and the activity of the transcription factors would pave the way for clarification of the molecular mechanism of circadian time-dependent processes.

In **Chapter 3**, I selected the insulin signaling pathway as a target of the analysis. It is known that insulin triggers multiple cellular signaling pathways including metabolism and transcriptional regulation upon secretion. In the insulin signaling pathway, a kinase Akt plays a crucial role in transmitting signaling information from the insulin.[36] However, because insulin triggers pathways other than Akt, the extent which Akt is sufficient to regulate the insulin signaling pathway is currently unknown. Optical stimulation using optogenetic Akt actuator, photoactivatable Akt (PA-Akt) system allows specific Akt activation upon light irradiation.[37] Perturbation with the PA-Akt system specifically activates Akt responsible signaling pathway. By globally quantifying transcripts by RNA-seq upon Akt selective activation, transcripts that are specifically regulated

by Akt is identified. Moreover, by integrating information from other types of molecular species (i.e. metabolites, proteins), a network of Akt dependent signaling pathway can be extracted. From this network, candidates of Akt regulated causative relationships would be identified. Thus, a combination of the molecule specific optical perturbation system (the PA-Akt system) and the global assessment of signaling molecules would enable the discovery of an unidentified regulation mechanism that Akt selectively activates.

Taken together, I aimed to demonstrate that optical perturbation system can serve as a platform for the transcriptional regulation analysis by performing these studies for both identifications of the candidate molecule and verification of the estimated regulation mechanism.

References

1. Wang, E. T. *et al.* Alternative isoform regulation in human tissue transcriptomes. *Nature* **456**, 470–476 (2008).
2. Guttman, M. *et al.* Ab initio reconstruction of cell type-specific transcriptomes in mouse reveals the conserved multi-exonic structure of lincRNAs. *Nat. Biotechnol.* **28**, 503–510 (2010).
3. Hobert, O. Gene Regulation by Transcription Factors and MicroRNAs. *Science* **319**, 1785–1786 (2008).
4. Chen, K. & Rajewsky, N. The evolution of gene regulation by transcription factors and microRNAs. *Nat. Rev. Genet.* **8**, 93–103 (2007).
5. Grimson, A. *et al.* MicroRNA Targeting Specificity in Mammals: Determinants beyond Seed Pairing. *Mol. Cell* **27**, 91–105 (2007).
6. Mukherjee, N. *et al.* Integrative Regulatory Mapping Indicates that the RNA-Binding Protein HuR Couples Pre-mRNA Processing and mRNA Stability. *Mol. Cell* **43**, 327–339 (2011).
7. Martinez, G. J. & Rao, A. Cooperative Transcription Factor Complexes in Control.pdf. **891**, 891–893 (2014).
8. Karczewski, K. J. *et al.* Cooperative transcription factor associations discovered using regulatory variation. *Proc. Natl. Acad. Sci. U. S. A.* **108**, 13353–13358 (2011).
9. Takahashi, K. & Yamanaka, S. Induction of Pluripotent Stem Cells from Mouse Embryonic and Adult Fibroblast Cultures by Defined Factors. *Cell* **126**, 663–676 (2006).
10. Tapscott, S. J. The circuitry of a master switch: Myod and the regulation of skeletal muscle gene transcription. *Development* **132**, 2685–2695 (2005).
11. Farmer, S. R. Transcriptional control of adipocyte formation. *Cell Metab.* **4**, 263–273 (2006).
12. Kojima, S., Shingle, D. L. & Green, C. B. Post-transcriptional control of circadian rhythms. *J Cell Sci* **124**, 311–320 (2011).
13. Alwine, J. C., Kemp, D. J. & Stark, G. R. Method for detection of specific RNAs in agarose gels by transfer to diazobenzyloxymethyl-paper and hybridization with DNA probes. *Proc. Natl. Acad. Sci.* **74**, 5350–5354 (1977).
14. Morley, A. A. Digital PCR: A brief history. *Biomol. Detect. Quantif.* **1**, 1–2 (2014).
15. Livak, K. J. & Schmittgen, T. D. Analysis of relative gene expression data using real-time quantitative PCR and the 2-ΔΔCT method. *Methods* **25**, 402–408 (2001).
16. Alam, J. & Cook, J. L. Reporter genes: Application to the study of mammalian gene transcription. *Anal. Biochem.* **188**, 245–254 (1990).
17. Paley, M. A. & Prescher, J. A. Bioluminescence: a versatile technique for imaging cellular and molecular features. *Med Chem Commun* **5**, 255–267 (2014).
18. de Wet, J. R., Wood, K. V, DeLuca, M., Helsinki, D. R. & Subramani, S. Firefly luciferase gene: structure and expression in mammalian cells. *Mol Cell Biol* **7**, 725–737 (1987).
19. Lorenz, W. W., McCann, R. O., Longiaru, M. & Cormier, M. J. Isolation and expression of a cDNA encoding Renilla reniformis luciferase. *Proc. Natl. Acad. Sci. U. S. A.* **88**, 4438–42 (1991).
20. Dixon, A. S. *et al.* NanoLuc Complementation Reporter Optimized for Accurate Measurement of Protein Interactions in Cells. *ACS Chem. Biol.* **11**, 400–408 (2016).
21. Sultan, M. *et al.* of the Human Transcriptome. *Science* **685**, 956–960 (2008).
22. Schena M, Shalon D, Dabis RW, B. P. Quantitative monitoring of gene expression patterns with a complementary DNA microarray. *Science* **270**, 467–470 (1995).
23. Mortazavi, A., Williams, B. A., McCue, K., Schaeffer, L. & Wold, B. Mapping and quantifying mammalian transcriptomes by RNA-Seq. *Nat. Methods* **5**, 621–628 (2008).

24. Adamson, B. *et al.* A Multiplexed Single-Cell CRISPR Screening Platform Enables Systematic Dissection of the Unfolded Protein Response. *Cell* **167**, 1867-1882.e21 (2016).
25. O'Connell, D. J. *et al.* Simultaneous Pathway Activity Inference and Gene Expression Analysis Using RNA Sequencing. *Cell Syst.* **2**, 323–334 (2016).
26. Fire, A. *et al.* Potent and specific genetic interference by double-stranded RNA in *Caenorhabditis elegans*. *Nature* **391**, 806–811 (1998).
27. Wang, T., Wei, J. J., Sabatini, D. M. & Lander, E. S. Genetic Screens in Human Cells Using the CRISPR-Cas9 System. *Science* **343**, 80–84 (2014).
28. Ryu, H. *et al.* Integrated Platform for Monitoring Single-cell MAPK Kinetics in Computer-controlled Temporal Stimulations. *Sci. Rep.* **8**, 11126 (2018).
29. Boyden, E. S., Zhang, F., Bamberg, E., Nagel, G. & Deisseroth, K. Millisecond-timescale, genetically targeted optical control of neural activity. *Nat. Neurosci.* **8**, 1263–1268 (2005).
30. Kennedy, M. J. *et al.* Rapid blue-light–mediated induction of protein interactions in living cells. *Nat. Methods* **7**, 973–975 (2010).
31. Komatsu, T. *et al.* Organelle-specific, rapid induction of molecular activities and membrane tethering. *Nat. Methods* **7**, 206–208 (2010).
32. Roth, B. L. DREADDs for Neuroscientists. *Neuron* **89**, 683–694 (2016).
33. Kamei, Y. *et al.* Infrared laser–mediated gene induction in targeted single cells *in vivo*. *Nat. Methods* **6**, 79–81 (2009).
34. Hirsch, S. M. *et al.* FLIRT: fast local infrared thermogenetics for subcellular control of protein function. *Nat. Methods* **15**, 921 (2018).
35. Dibner, C., Schibler, U. & Albrecht, U. The Mammalian Circadian Timing System: Organization and Coordination of Central and Peripheral Clocks. *Annu. Rev. Physiol.* **72**, 517–549 (2010).
36. Kahn, S. E., Hull, R. L. & Utzschneider, K. M. Mechanisms linking obesity to insulin resistance and type 2 diabetes. *Nature* **444**, 840–846 (2006).
37. Katsura, Y. *et al.* An optogenetic system for interrogating the temporal dynamics of Akt. *Sci. Rep.* **5**, 1–10 (2015).

Chapter 2

Transcriptional characteristics in circadian clock synchronization by ultraviolet irradiation

2-1. Introduction

2-1-1. The circadian clock system

The circadian clock is a cell-autonomous timing system with the oscillation of 24 hours period that regulates cellular global gene expression of living organisms.[1] One of the characters of the circadian clock is that every single cell has an ability to synchronize its circadian phase in response to external factors including stress inducing stimulations, thereby exhibiting cellular homeostasis for cellular adaptation to the surrounding environment.[2,3] A dysfunction of circadian clock leads to an arrhythmic behavior and sleeping disorders thus it is essential for appropriate homeostasis of a living system. According to early works on the circadian clock, the circadian clock is defined as an autonomous system with the following three fundamental properties.

1) Oscillation of rhythm is approximately 24 h period.
2) A period of oscillation is temperature compensated.
3) A phase of oscillation is capable to be entrained by external stimulation.

Among these features, entrainment (synchronization of the phase and the period of the circadian clock to those of external oscillation) has attracted attention because synchronization of circadian clock maintains appropriate daily time-keeping function. It is estimated that a property of circadian clock to synchronize an internal rhythm to that of environment was achieved at the early stage of evolution of life.[4] In fact, circadian clock is widely preserved in variety of species including prokaryote; cyanobacteria (*Synechococcus elongatus*),[5,6] and eukaryotes; red bread mold (*Neurospora crassa*),[7] insects (*Drosophila melanogaster*),[8] and vertebrates (*Mus musculus*, *Homo sapience*).[9,10] Thus, synchronization to external cycle is essential for living organisms.[11]

In a mammalian circadian system, almost every cell in the organism has its own circadian clock, although a hierarchical organization of the synchronization exists.[12,13] A master clock exists in the suprachiasmatic nucleus (SCN), which is located at above the optical chiasm in the hypothalamus, regulates circadian clock in peripheral tissues and cells (named peripheral clocks).[14] The master clock in the SCN synchronizes to the geological day-and-night cycle sensed by the eyes and transmits a synchronization signal to the peripheral clocks (**Figure 2-1**).[15,16] Despite the fact that the clock in the SCN functions as a synchronizer of peripheral clocks, peripheral clocks are also capable to synchronize by an external stimulation.[17]

Up to date, a molecular mechanism underlying synchronization is yet to be fully elucidated. One of the difficulties is that circadian clock is capable to be synchronized with diversities of an

external cue. In addition, each stimulation resets the clock by different molecular machinery.[18–20] Hence, it is unclear whether any general principle for synchronization of circadian clock exists or not.

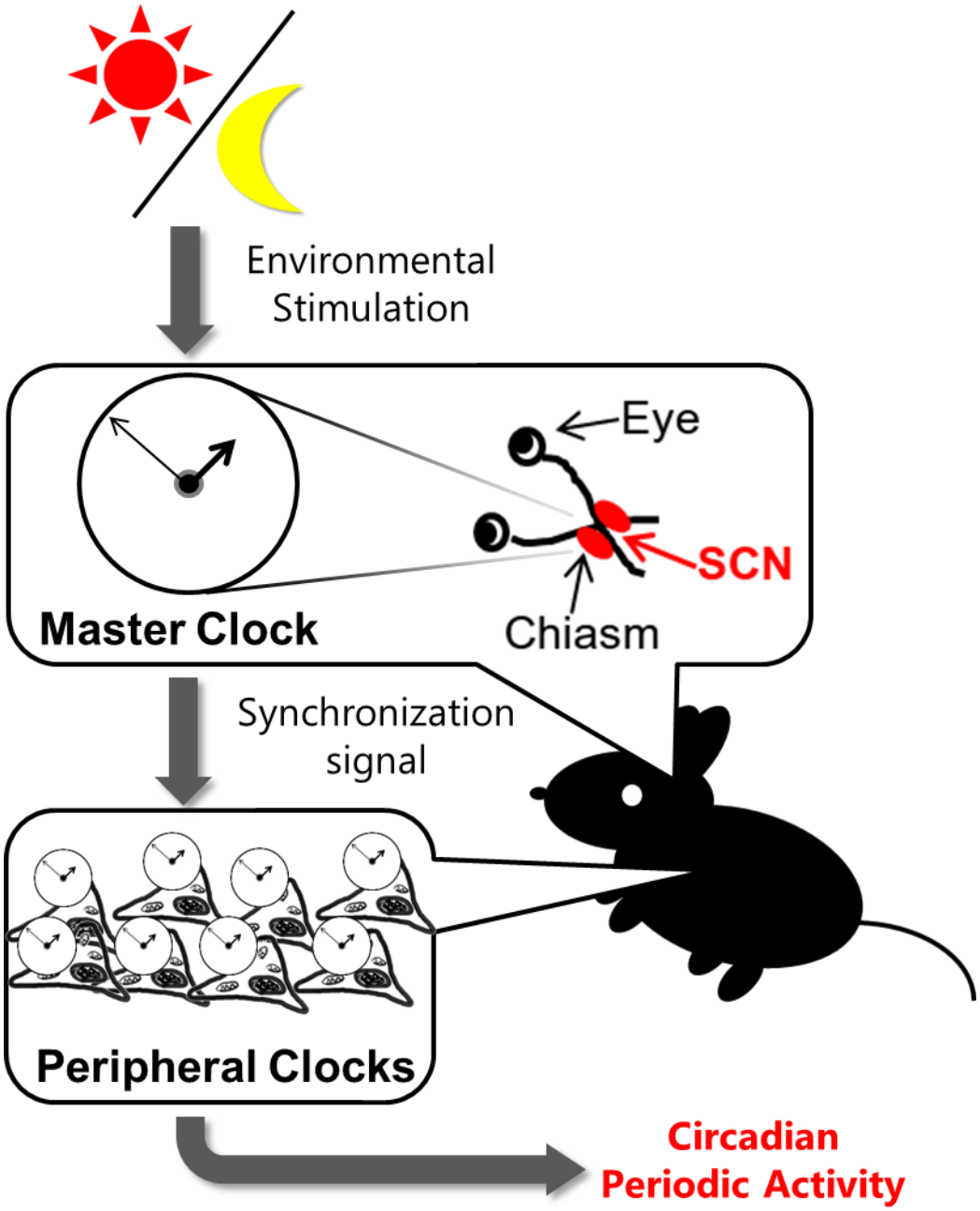

Figure 2-1. Hierarchical organization of the circadian clock system.
An environmental light signal is transmitted to the SCN and synchronizes a circadian clock of SCN. The circadian clock in the SCN then synchronizes the circadian clock in peripheral tissues and cells. The daily rhythmic activity in tissue is controlled by the peripheral clocks.

2-1-2. Molecular mechanism of circadian clock and stress response

Molecular level understanding of the adaptation process including circadian clock synchronization is crucial for understanding the interplay among circadian clock components and stress response systems. For circadian clock system, oscillation of the clock is maintained by positive and negative transcriptional–translational feedback loops driven by circadian transcription factors, represented by BMAL1 and CLOCK. Heteroduplex of BMAL1 and CLOCK regulates gene expressions of negative regulating clock gene *Per* and *Cry*, which are in turn accumulated in the nucleus to suppress trans-activation by BMAL1/CLOCK (**Figure 2-2**).[21] Since clock genes *Per* and *Cry* are expressed in a circadian timing manner, gene expression regulation by BMAL1/CLOCK is an important feature for the synchronization process.[22] Therefore synchronization process involves activation of transcriptional activity of circadian transcription factors and/or regulation of clock genes.

So far, proteotoxic stresses such as heat shock (HS) or reactive oxygen species (ROS) is known to trigger a reset of circadian timing via protein-protein interactions between BMAL1 and HSF1, a central transcription factor for the heat-shock response (HSR) pathway.[23–25] Other reports also identified a clock-driven stress protection system, which is regulated by interplay between clock components and transcription factors for the stress response pathways, including HSF1 and anti-oncogene transcription factor, p53.[26,27] For HSF1, recent work demonstrated that proteotoxic stress-induced activation of HSF1 was involved in a reset of circadian clock through a short-term elevation of *Per2* mRNA expression.[25] Moreover, it was suggested that the transcriptional activation of HSF1 corresponds with a protein-protein interaction of HSF1 with circadian transcriptional factor BMAL1.[24] Furthermore, in p53 mediated anti-genotoxic response, trans-activation products of BMAL1/CLOCK, *Cry1*, *Cry2,* and *Per2* have a function in sensitivity of p53 to stresses.[28,29] Recent findings suggest that the activity of anti-genotoxic pathway may possibly be affected by HSF1, possessing a question that those two pathways cooperatively act for cellular protection.[30,31]

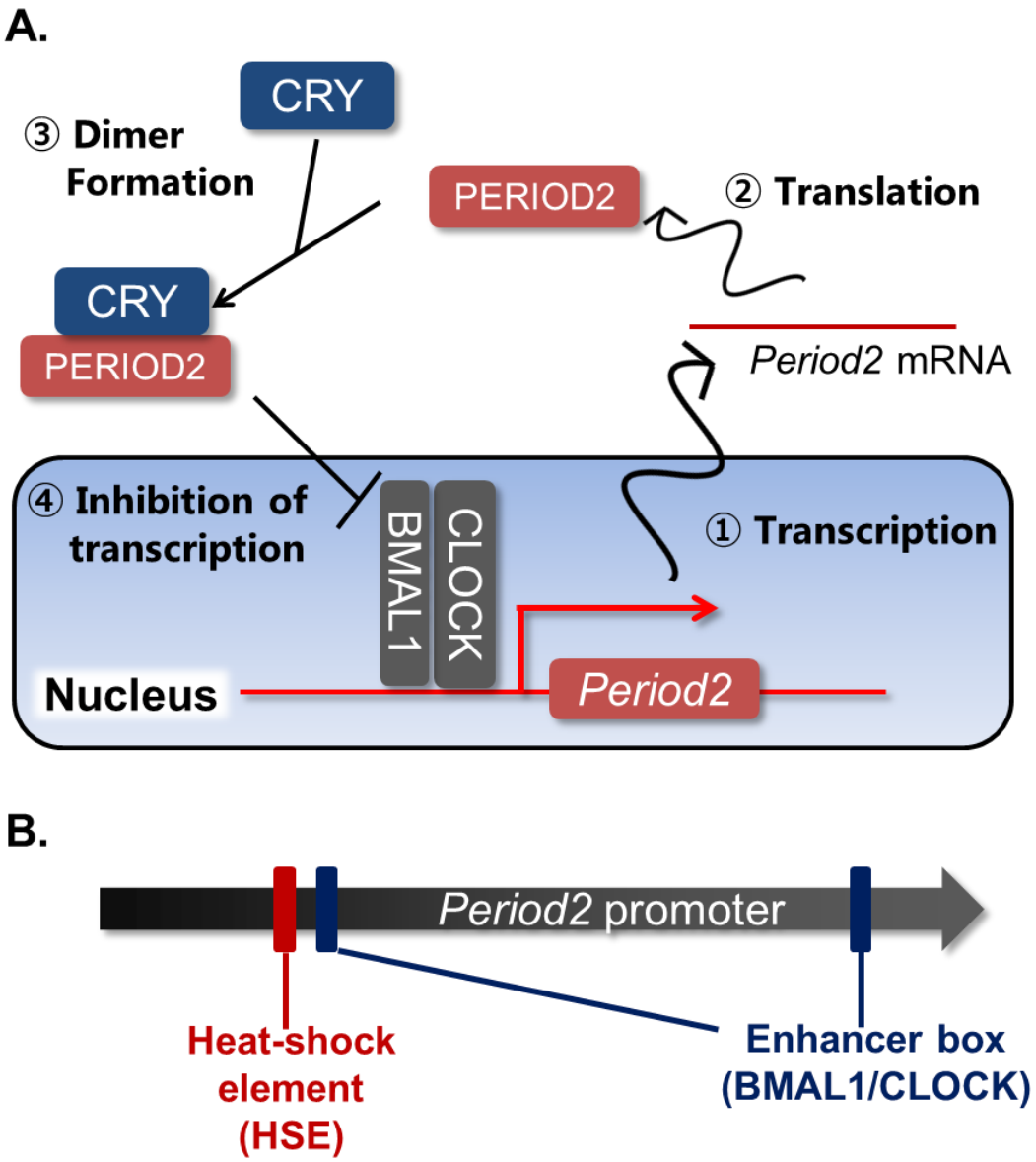

Figure 2-2. Generation of circadian periodic oscillation.
(A) A transcriptional-translational feedback loop consisting of circadian transcription factors, BMAL1 and CLOCK, and repressors of transcriptional activity, CRY, and PERIOD2. *Period2* mRNA is regulated by BMAL1 and CLOCK. Transcribed and translated PERIOD2 protein, in turn, forms a heterodimer with CRY. The heterodimer represses BMAL1 activity, resulting in repression of its own transcript. (B) Schematics of the promoter region of *Period2*. A binding site for transcription factors, BMAL1/CLOCK, HSF1 and p53 exists on the *Period2* promoter.

2-1-3. Heat-shock response pathway

Heat-shock response pathway is one of the stress-responsive machinery that regulate a protection system against proteotoxic stresses. The main function of the heat-shock response pathway is refolding of damaged proteins by protein chaperones such as heat-shock protein 40 (Hsp40) and heat-shock protein 70 (Hsp70).[32] HSF1 modulates the expression of these protein chaperons at a transcription level. Thus, HSF1 plays a central role in the heat-shock response pathway.[33,34]

In a non-stressed condition, HSF1 forms a heterodimer with a protein chaperone, heat-shock protein 90 (Hsp90).[35] Upon proteotoxic stress, Hsp90 dissociates with HSF1 to function as a protein chaperone to help a refolding of damaged proteins. As a consequence, HSF1 is released from the heterodimer complex and translocates to the nucleus to form a homotrimer that binds to a heat-shock element (HSE).[36] An HSE sequence is located in the promoter region of heat-shock responsive genes, hence their transcription levels are increased upon activation of HSF1 (**Figure 2-3**).

Recent studies in transcriptional activity of HSF1 do not focus just on the heat-shock response pathway but also on other signaling pathways.[37] Pieces of evidence arose that HSF1 also functions cooperatively with other stress response pathways, such as the Nrf2-Keap1 anti-oxidant pathway,[38] the NF-kappa B signaling pathway,[39] and the p53 DNA damage response pathway.[30,31,40] For the interaction with the circadian clock system, HSF1 was identified to function as a circadian transcription factor in the liver circadian clock.[27,41] It is noteworthy that p53, an interactor of HSF1, was reported to act as a repressor of *Per2* gene expression by competitive binding to its promoter, thereby modulating a circadian oscillation.[42] These findings suggest a role of the stress response pathway for the modulation of circadian transcriptional regulation.

Despite the fact that HSF1 and p53 functions cooperatively to regulate a circadian transcription in stress responses, there is no evidence for interplay between the heat-shock response pathway and p53 DNA damage response to modulate the circadian system.

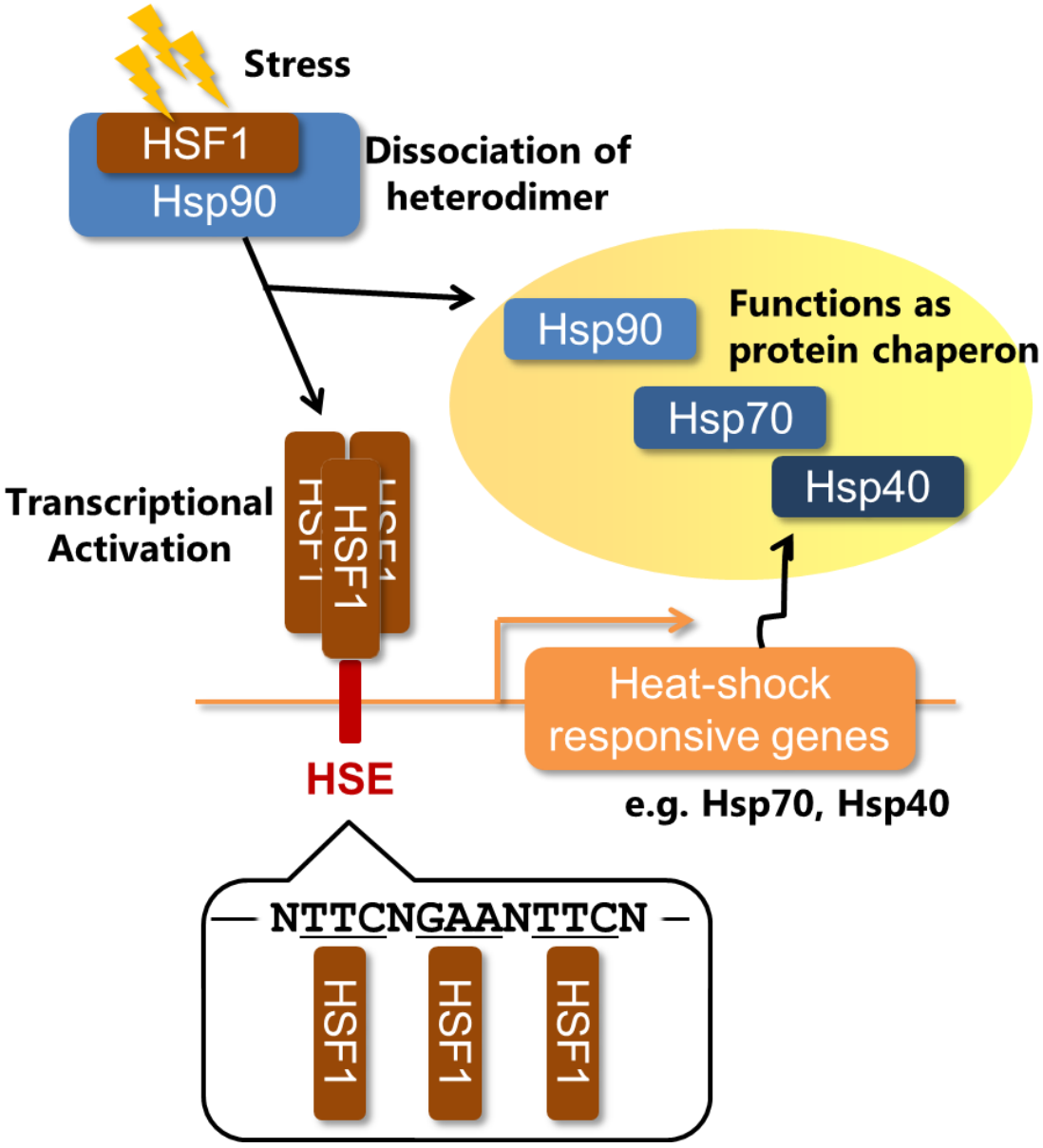

Figure 2-3. Activation of HSR after proteotoxic stress.
Hsp90-HSF1 heterodimer senses the proteotoxic stress to initiate the activation of HSR. Upon stress, HSF1 is released from the complex and translocates to the nucleus to form a homotrimer. Homo-trimer binds to an HSE sequence and regulates the transcription of heat-shock responsive genes. Transcribed heat-shock responsive genes functions as a protein chaperone to refold a damaged protein.

2-1-4. Purpose of this study

Adaptation to stress mediated by clock-controlled genes triggered by the circadian clock system is especially important for cellular protection systems since clock-controlled genes comprise around 40% of total mRNA, including stress responsive genes.[43] Indeed, disruption of clock components which leads to altered expression of circadian components and circadian controlled genes results in proliferation disorders and tumor progression by altered sensitivity to proteotoxic and genotoxic stimulation.[44,45]

Because the abundance of the circadian clock components or degree of interactions between the components possibly varies according to the circadian time, understanding of circadian clock-dependent stress adaptation responses requires analysis of their circadian time-dependency. Therefore, in this chapter, I examined the circadian time-dependent molecular process in response to cellular stress, especially at the early stage post genotoxic damage induced by ultraviolet (UV) irradiation to characterize circadian time-dependent adaptation towards the stress stimulation. For this purpose, I employed UV as an optical perturbation system to deliver stimulation in a high temporal resolution manner. By measuring time-dependency of the response of clock gene transcriptional regulation and activation of transcriptional modulators, temporal aspect of the circadian clock synchronization upon UV irradiation is expected to be clarified.

2-2. Materials and methods

2-2-1. Plasmid construction

Generation of a construct for the mouse *Per2* promoter-driven destabilized luciferase reporter (Per2-Luc) and destabilized SLR red luciferase (Toyobo, Japan) reporter connected with 3× HSE (HSE-SLR) are described in the previous research.[25] Mutants of mouse Per2-Luc was developed by site-directed mutagenesis. Bioluminescence reporter expression vectors for HSE or a p53-responsive element (p53RE) consensus sequence in the mouse *Per2* promoter were generated from the Per2-Luc probe by PCR amplification and enzymatic digestion followed by ligation of the DNA fragments.

For split luciferase complementation assays, split fragments of Emerald Luciferase (ELuc) cDNA (Toyobo, Japan), namely, N-terminal fragment of luciferase (N-Luc, 1-415 amino acid residues) and C-terminal fragment of luciferase (C-Luc 393-542 amino acid residues) were used. Full-length mouse p53 was inserted to the downstream of the C-terminal (ELucC) on pcDNA3.1 vector (Invitrogen). Vectors for ELuc N-terminal fragment fused mouse HSF1 was constructed in previous literature. [25]

2-2-2. Cell culture

Mouse fibroblast NIH3T3 cell (RIKEN cell bank, Japan), wild-type mouse embryonic fibroblast (MEFs) cell, BMAL1$^{-/-}$ cell, HSF1$^{-/-}$ MEFs cell,[46] p53$^{-/-}$ MEFs cell,[47] plat E cell were used. All cell-lines were cultivated with Dulbecco's modified eagle medium (D-MEM, Nacalai tesque) supplemented with fetal bovine serum (FBS, Gibco) and 1% penicillin/streptomycin (Gibco).

Transfection of a probe DNA plasmid to cultured cells was performed using TransIT-LT1 transfection reagent (Mirus bio) following manufacturer's protocol. For a generation of a stable cell line expressing the Per2-Luc or the HSE-SLR reporter, retrovirus infection was conducted using a retrovirus produced in a plat-E cell using polybrene (hexadimethrine bromide, the final concentration of 0.24 mg/ml). Stable cell-lines for all the other reporter gene assays were generated through an anti-biotic selection by hygromycin B after transfection of the probes.

2-2-3. Real-time bioluminescence monitoring and data processing

Cells were synchronized with UV light (254 nm cross-linker, UVP) irradiation. As to induce a

genotoxic stimulation to the cells, UV in the shorter wavelength (UV-C) was selected.[48] For the positive control of synchronization, dexamethasone treatment (10 nM, 2 h) was used. Real-time bioluminescence monitoring was conducted with Kronos dio (ATTO, Japan). A culturing medium supplemented with 0.1 mM D-Luciferin (Wako, Japan) were used. The acquisition intervals of 30 min for Per2-Luc and 10 min for other reporter experiments.

"Deviation from the moving average" of the assay represents that the raw values were subtracted a moving average according to the program within the detector (Kronos; ATTO, Japan). The detrended values were further normalized by using maximum peak intensities over recorded values for the comparison. Circadian rhythmicity and period were calculated by the cosinor method using "Cosinor" software downloaded from the Circadian Rhythm Laboratory Software home page (http://www.circadian.org/softwar.html) based on detrended and normalized luminescent profiles.

Real-time bioluminescence single-cell imaging was conducted under BX-61 bioluminescence microscope (Olympus, Japan). Single-cell tracking for the analysis of luminescent profile of each cell was performed using TrackMate plugin in a Fiji software,[49] according to the developer's protocol. Values were normalized to maximum peak intensities over time.

2-2-4. Immunoblot and immunoprecipitation assays

Cells cultivated in a culture dish were exposed to UV-C light (254 nm, 10 J/m^2) and restored back to incubation until a predetermined time point of the sample collection. At the sampling time point, cells were washed twice with ice-cold phosphate-buffered saline (PBS) and lysed with an NP-40 lysis buffer {10 mM Tris-HCl (pH = 7.4), 150 mM NaCl, 5 mM EDTA, 50 mM NaF and 0.5% NP-40} supplemented with a protease inhibitor cocktail (cOmplete, Roche) and a phosphatase inhibitor cocktail (Phosstop, Roche). Lysed sample was centrifuged at 4^{o}C at 15,000 rpm for 20 min. For immunoprecipitation assays, supernatant after centrifuge was collected and a Triton-X 100 containing lysis buffer was added to dilute the sample to 1 mL and incubated with protein-G sepharose for an over-night. The resultant products were separated to incubate with the anti-HSF1 antibody (Cell Signaling Technologies) or anti-p53 antibody (SantaCruz technologies) with protein G-sepharose for 6 hours at 4^{o}C. Protein sepharose beads were collected and washed with PBS buffer for three times and diluted with lysis buffer. The loading sample for SDS polyacrylamide gel electrophoresis (SDS-PAGE) was prepared by adding 0.2 equivalent of 5x Sampling buffer {250 mM Tris-HCl (pH7.6), 10% SDS, 25% Glycerol, 5% 2-mercaptoethanol, 0.02% bromophenol blue} to the supernatant of the centrifuged mixture. Immunoblotting was performed at 4^{o}C overnight condition using specific primary antibodies against a target protein. A primary antibody against BMAL1,[50] HSF1, Hsp70

(Cell Signaling Technologies), p53 and βactin (Abcam) were used. Anti-rabbit IgG and anti-mouse IgG antibodies labeled with horseradish peroxidase (GE Healthcare) were used as secondary antibodies. Chemiluminescence from the immunostained bands was detected with ImageQuant LAS4000 Mini (GE Healthcare). The band intensities were quantified using Fiji software.

2-2-5. Chromatin immunoprecipitation

NIH3T3 cells cultivated in a culture dish were exposed to UV-C light (10 J/m^2) and restored back to incubation until a predetermined time point of the sample collection. At the collection point, cells were washed with PBS (-) twice and fixed with 1% paraformaldehyde at room temperature for 5 min. The reaction was quenched with 1M glycine and centrifuged to collect the cells. Cells were treated with RIPA buffer and incubated on ice for 20 min and subjected to sonication for at least 1 min for each sample. The supernatant after centrifuge was collected and a Triton-X 100 containing lysis buffer was added to dilute the sample to 1 mL and incubated with protein-G sepharose for an over-night. The resultant products were separated to incubate with anti-HSF1 antibody, anti-p53 antibody or a mouse IgG (SantaCruz technologies) with protein G-sepharose for 6 hours at 4ºC. Protein sepharose beads were collected and washed with TritonX-100 buffer for three times and reverse crosslinking buffer (62.5 mM Tris-HCl pH6.8, 200 mM NaCl, 2% SDS and 10 mM DTT) was added and the sample was vortexed and incubated at 65ºC for an overnight. DNA fragments were collected by phenol-chloroform extraction followed by ethanol precipitation.

2-2-6. Quantitative PCR

For quantification of a transcription factor bound DNA, a quantitative PCR against mouse *Per*2 promoter sequence using chromatin immunoprecipitated samples were performed. The following primers were used: p53RE/E-box2, 5’- CAG GTT CCG CCC CGC CAG TAT-3’, and, 5’ – GTC GCC CTC CGC TGT CAC ATA G -3’; HSE1, 5’- GCC TCC TTT CCA TTC CTG -3’, and, 5’- GGA GAA GGC AAG CTT GTC -3’; HSE2, 5’- GAA GAC GTG ACA AGC TTG C -3’, and, 5’- CTG TCC AAA GGG TCA AAG G -3’, E-Box5, 5’- CTC TGT AGG GTG GAG CGG CGA -3’, and 5’- ATC CCC ACT GCT CCT TCG CAC -3’, and Mdm2, 5’- GTT GAC TCA GCT CTT CCT GTG G -3’, and, 5’- GGC TGC GGA AAC GGG GCA GCG -3’. The DNA fragments were amplified using (THUNDERBIRD SYBR qPCR Mix (TOYOBO, Japan) following manufacturer's protocol. The fluorescence amplification curve was detected by a Thermal Cycler Dice Real Time System II (TakaraBio, Japan) and the quantification was

performed from independent ChIP experiments. The values represent % input compared to the control, which is the total amount of DNA subjected to the analyses, and the value for this control was set to 100%.

2-2-7. Transcriptome data analysis for UV and oxidative stress-regulated genes

Microarray data for UV irradiated MEFs and hydrogen peroxide-treated NIH3T3 cells were downloaded from the Gene Expression Omnibus (GEO; http://www.ncbi.nlm.nih.gov/geo/) under accession number GSE50930 and GSE47955.[24,51] From the data, processed RMA values were used in further analysis. Gene expressions were normalized to that of no stimulated sample and abundance changes were calculated as $\log_2$ fold change compared to stimulation time 0 min. To address for the reliability of the data, UV regulated genes with inconsistent expression trend in the initial three-time points of data sets (10, 30, 60 min) were omitted from the analysis. Data were treated with custom written MATLAB (Math Works) code and R (https://www.R-project.org). For a depiction of Venn diagram, "VennDiagram" package in R was used.[52] Pathway maps for UV stimulated gene expression profiles were depicted using PathVisio software[53,54] with pathway information from WikiPathways.[55,56]

2-2-8. Statistical analyses

All the experiments were conducted with specifically chosen sample size with appropriate tests. Error bars represent the standard deviation as indicated in the legends. Statistic values (p values and *F* values) were obtained from two-sided t-tests or one-way ANOVA. All statistical testing was performed with R.

2-3. Results

2-3-1. UV irradiation synchronizes cellular circadian clocks via a heat-shock response pathway

First, I evaluated the optimal dose of UV irradiation to synchronize circadian clock as mammalian cellular clock model responding to the genotoxic stress. For this purpose, NIH3T3 fibroblasts harboring *Period*2 (*Per*2) promoter-driven firefly luciferase (Per2-Luc) reporter was used to analyze real-time temporal Per2-Luc profiles upon irradiation with various strength of UV stimulation (254 nm). Rhythmic Per2-Luc pattern was observed by UV strengths between 2 to 20 J/m^2 and most evident at 10 J/m^2, indicating that cellular stress by UV irradiation with appropriate dose triggers synchronization of circadian clocks (**Figure 2-4A** and **Table 2-1**). Additionally, dose-dependent surge of Per2-Luc luminescence after UV irradiation was observed between strength of 2 to 30 J/m^2 and the peak intensity decreased at the dose over 50 J/m^2, indicating that Per2-Luc responded to genotoxic stress in a dose-dependent manner before it reached a critical dose (30~ J/m^2) (**Figure 2-4B**). Since viability of cells after the exposure significantly drops beyond the strength of 30 J/m^2 (**Figure 2-5**), from here, I employed 10 J/m^2 as an appropriate dose for genotoxic stimulation to induce a circadian response and cellular protection system.

Stimulation	Period [h]
2 J/m^2	25.3 ± 0.5
5 J/m^2	25.3 ± 0.8
10 J/m^2	24.8 ± 0.7
15 J/m^2	22.3 ± 1.2
20 J/m^2	21.1 ± 1.9
30 J/m^2	Not periodic
50 J/m^2	Not periodic
100 J/m^2	Not periodic

Table 2-1. Dose-dependent synchronization of circadian clocks.
Per2-Luc profile of NIH3T3 stimulated with various strength of UV was recorded, as in **Figure 2-4**, and the period was determined from the temporal profiles of Per2-Luc signal. *N* = 3, +/-: SD.

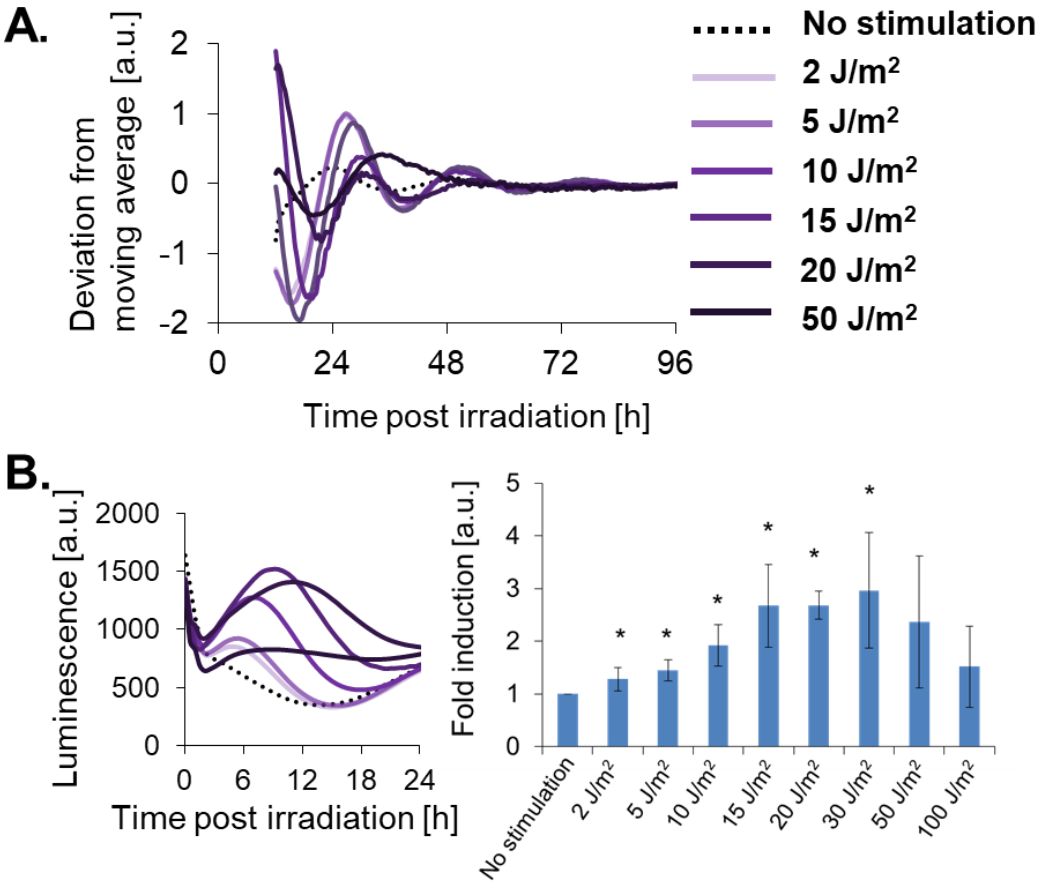

Figure 2-4. Dose-dependent profiles of Per2-Luc
Per2-Luc profiles of NIH3T3 stimulated with various strength of UV were recorded. (A) Detrended profiles of Per2-Luc stimulated with different doses of UV irradiation. (B) The initial surge of Per2-Luc after UV irradiation represented by Per2-Luc profile of 0 to 24 hours post irradiation. Relative area under the curve to no stimulation is plotted for various doses of UV irradiation. *: p<0.05, *N* = 3, +/-: SD.

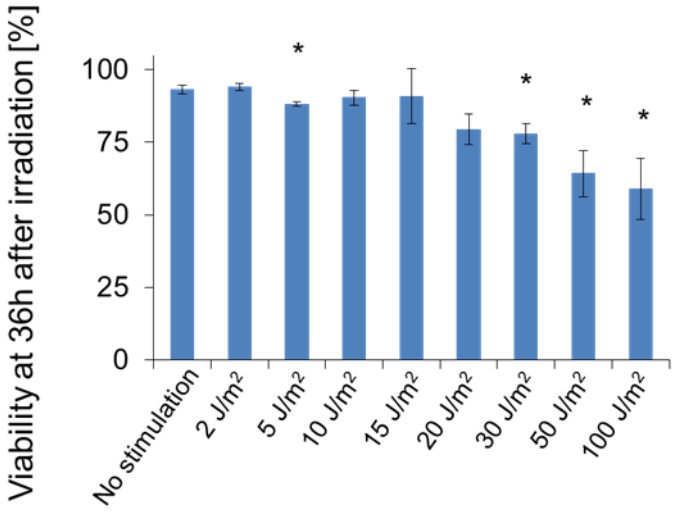

Figure 2-5. Cell viability assay after UV irradiation.
Cells were subjected to trypan blue cell death assay at 36 hours post irradiation with various doses of UV irradiation. *: p<0.05, *N* = 3, +/-: SD.

Based on the recent findings that HSR pathway is responsible for circadian clock synchronization by HS and ROS induced cellular stress,[24,25] I investigated the role of HSR in UV-triggered clock synchronization. In these previous papers, the fundamental role of HSF1 to modulate *Per*2 expression is described. Thus, I analyzed the response of Per2-Luc reporter in wild-type and HSF1$^{-/-}$ MEFs after UV irradiation. Upon stimulation, Per2-Luc luminescence began to increase within 6 h post irradiation and then exhibited circadian oscillation in the wild-type cells. Whereas in HSF1$^{-/-}$ cells, no significant initial response was observed (**Figure 2-6**). Also, no circadian oscillation of Per2-Luc is observed with UV irradiation in HSF$^{-/-}$ cells (**Figure 2-7**). Importantly, dexamethasone (Dex) treatment synchronized both wild-type and HSF1$^{-/-}$ cells, indicating that clock maintenance function remains present in HSF1$^{-/-}$ cells. These results demonstrate that HSF1 controlled HSR is essential for UV-triggered clock synchronization by inducing a synchronous surge of *Per*2 expression after UV stimulation.

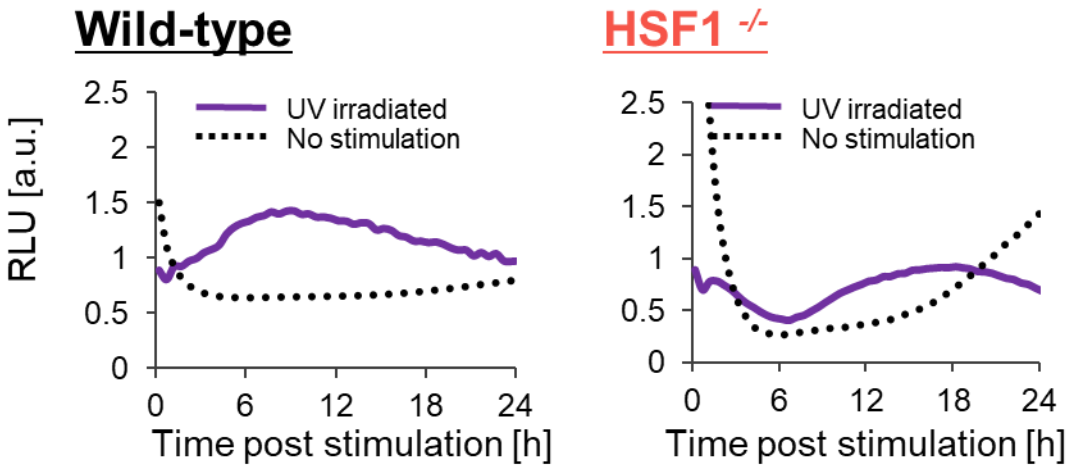

Figure 2-6. Per2-Luc initial surge in wild-type and HSF1$^{-/-}$ MEFs.
Per2-Luc profiles after UV irradiation (10 J/m^2) or no stimulation were observed in wild-type and HSF1$^{-/-}$ MEFs. Representative Per2-Luc profiles 0 to 24 h post irradiation is shown for each cell type.

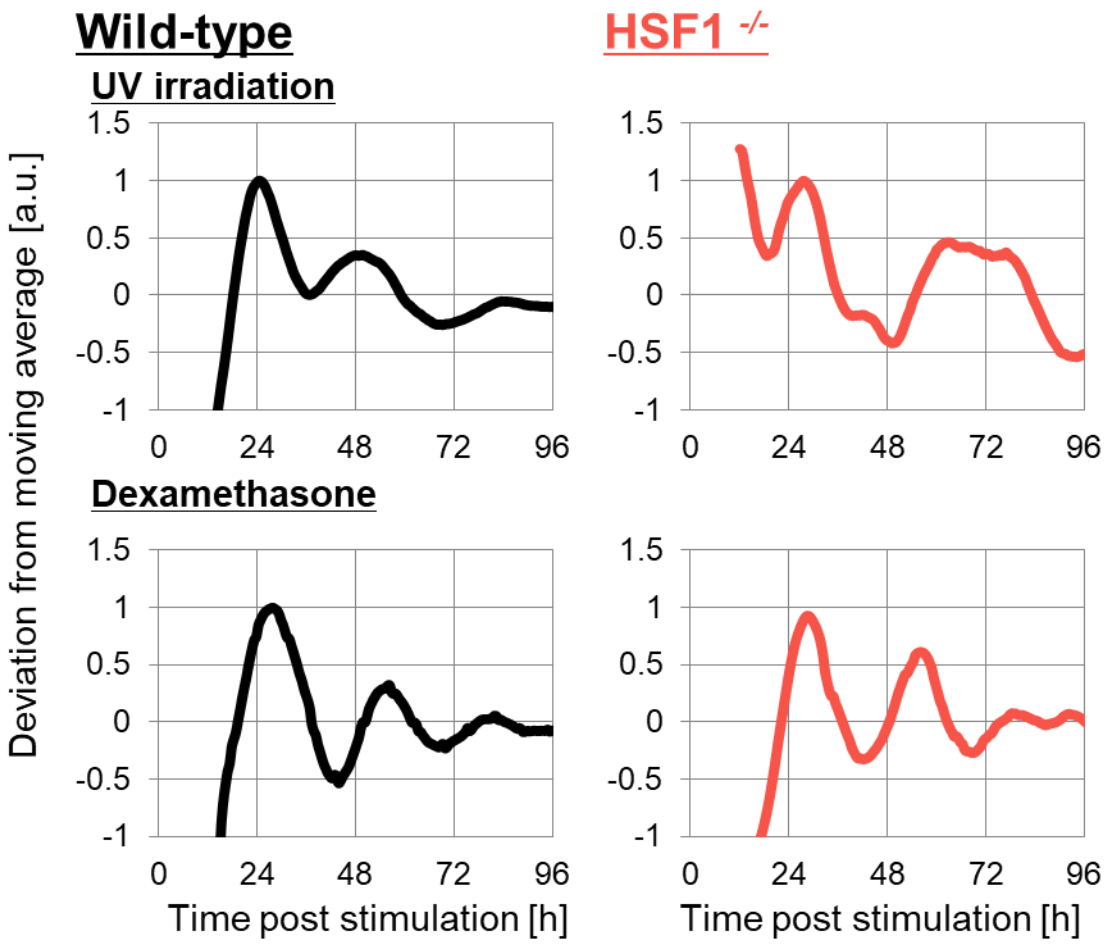

Figure 2-7. Per2-Luc oscillation in wild-type and HSF1$^{-/-}$ MEFs.
Per2-Luc profiles after UV irradiation (10 J/m^2) or Dex treatment (10 nM, 2 hours) were observed in wild-type and HSF1$^{-/-}$ MEFs. Representative detrended Per2-Luc profiles post stimulations are shown.

I next investigated whether HSR is activated upon UV irradiation or not. To this objective, I analyzed HSR activation by quantification of abundance change in HSF1 trans-activated gene product after the stimulation, both in a protein and mRNA levels. The protein abundance of HSR product, HSF1 and Hsp70 were acutely increased within 2 h post irradiation, suggesting that UV irradiation triggered activation of HSR transcriptional activity (**Figure 2-8**). HSF1 mediated trans-activation was confirmed by measurement of mRNA levels of targets of HSR, *Hsf1,* and *Hsp70*,[57] after the irradiation (**Figure 2-9**). mRNA levels of *Hsf1* and *Hsp70* increased within one hour after the irradiation, which is consistent with our findings that both HSF1 and Hsp70 protein levels increase the upon stimulation.

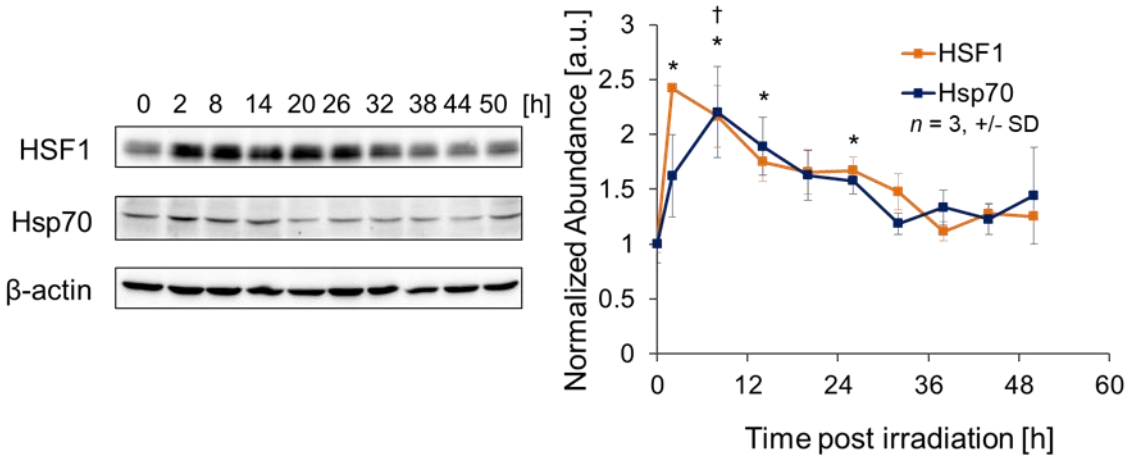

Figure 2-8. HSR protein abundance changes after UV irradiation.
Protein abundance of HSR proteins, HSF1 and Hsp70 were measured after UV irradiation. Band intensities were normalized to that of β-actin and further normalized to 0 h post irradiation. Relative abundance change is shown. N = 3, +/-: SD. *: p<0.05 for HSF1 abundance, †: p<0.05 for Hsp70 abundance. Two-tailed t-tests.

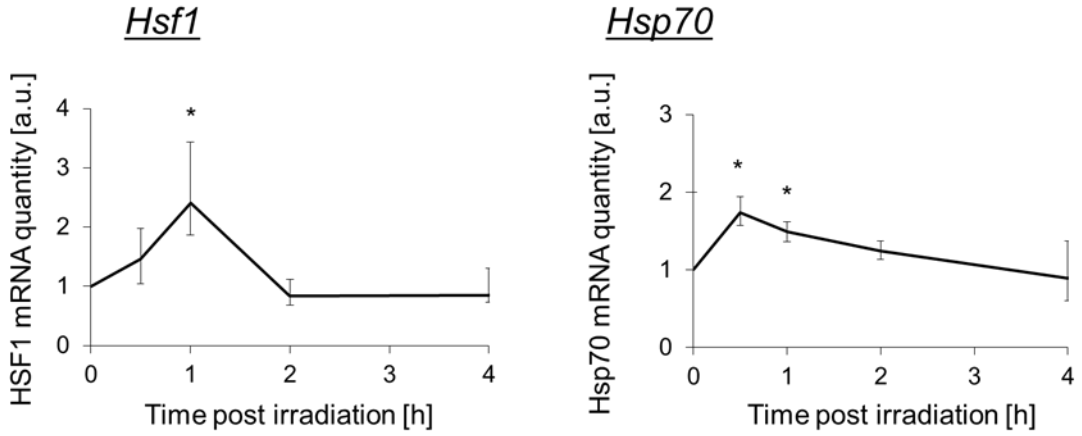

Figure 2-9. HSR mRNA abundance changes after UV irradiation.
mRNA abundance of HSR genes, HSF1 and Hsp70 were measured after UV irradiation by qPCR. Quantification was performed by ΔCt method, normalized to mRNA quantity of β-actin. Relative abundance change is shown. *N* = 3, +/-: SD. *: p<0.05, two-tailed t-tests.

Transcriptional activation of HSF1 was further confirmed by reporter gene assay of an HSE sequence, which is known to be bound by HSF1. I conducted bioluminescence imaging of HSE-driven railroad worm red luciferase (HSE-SLR) reporter after UV irradiation at single-cell level (**Figure 2-10**). An acute increase in each single cellular HSE-SLR luminescence was observed, suggesting that HSF1 activity is evoked synchronously after the irradiation. Since HSF1 activation occurred synchronously in each individual cell, this result provides the evidence indicating that HSF1 activation is a critical molecular event in UV-triggered clock synchronization.

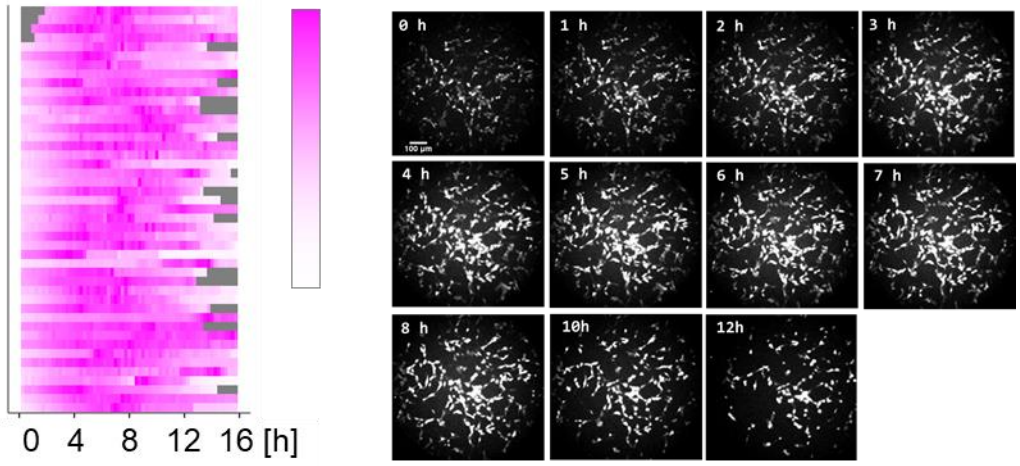

Figure 2-10. Single-cell measurement of HSE-SLR reporter after UV irradiation.
Single-cell luminescence properties of HSF1 responsive HSE-SLR was measured under luminescence microscope. A heat map represents relative intensity change over time. Each row in the heat map corresponds to each cell. Analyses were performed with TrackMate plugin in Fiji software. Representative images of analyzed data are shown. Scale bar: 100 μm.

To look for the molecular basis of HSF1 function on *Per*2 expression, mutagenesis assays were performed. Since mouse *Per*2 promoter carries two HSE sites namely HSE1 and HSE2 adjacent to the E-Box, I examined whether HSF1 trigger synchronous circadian *Per*2 expression after binding to those HSE post UV irradiation (**Figure 2-11**).

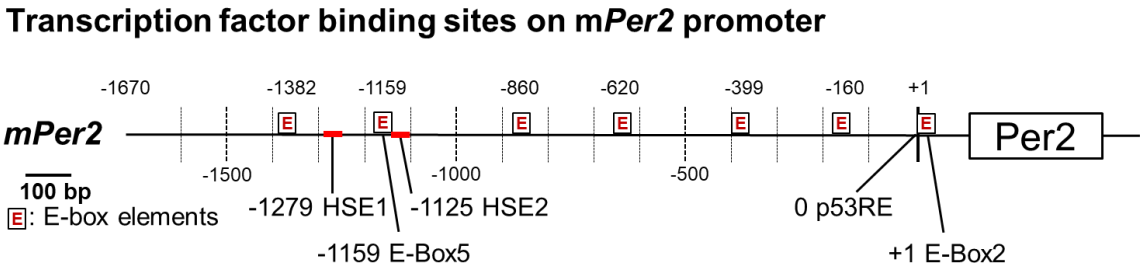

Figure 2-11. Schematics of the mouse *Per*2 promoter.
Schematic diagram representing major transcription factor binding sites on mouse *Per*2 promoter. E-Box: BMAL1/CLOCK, HSE: HSF1 and p53RE: p53. Numbers adjacent to each binding site indicates the distance from transcription starting site in base pairs.

To examine which HSE sites are required for UV-triggered circadian clock resetting, I performed mutagenesis reporter assay, which sequence of HSE sites of *Per2*-Luc were introduced with a point mutation. Then I analyzed the profile of mutagenetic *Per*2-Luc after UV exposure. NIH3T3 cells expressing native Per2-Luc or HSE-mutated Per2-Luc were stimulated with UV irradiation or Dex. The acute surge in native Per2-Luc after UV irradiation was

impaired dramatically in the HSE2 mutated Per2-Luc while HSE1 mutated Per2-Luc showed clear surge upon stimulation (**Figure 2-12**).

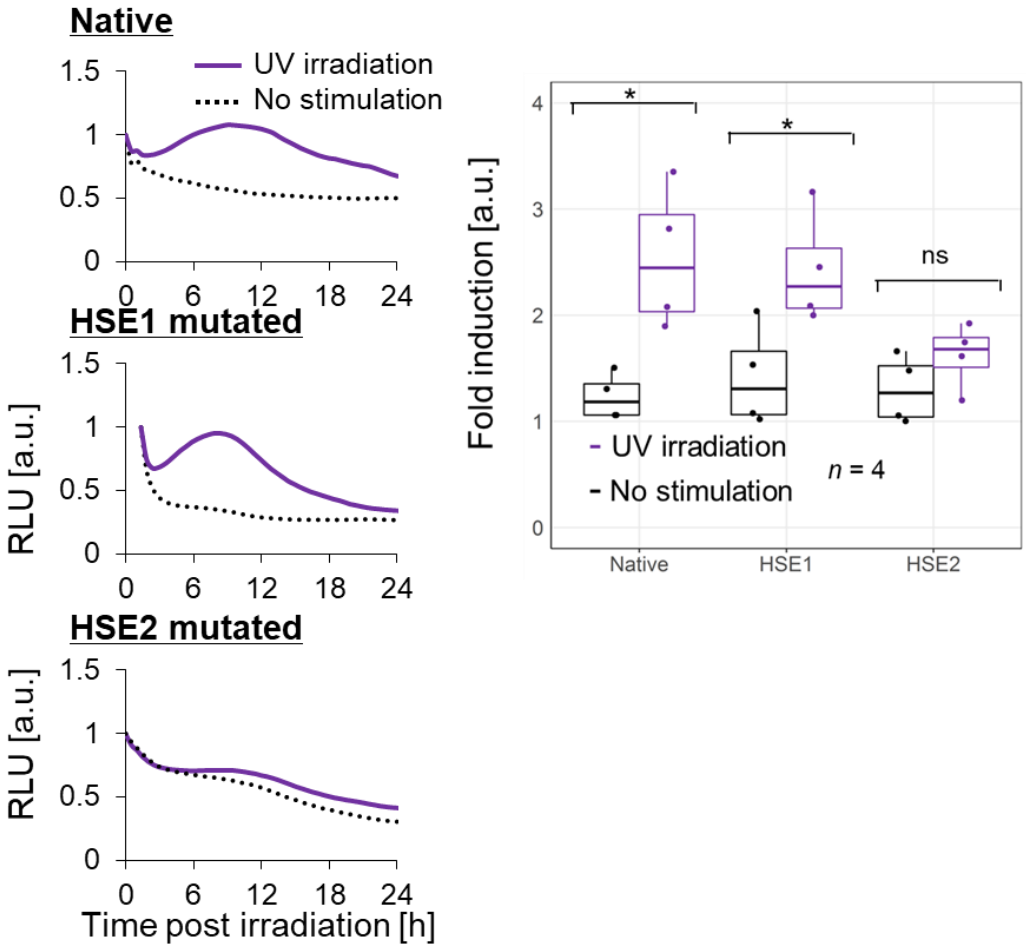

Figure 2-12. Initial surge of mutated Per2-Luc after UV irradiation.
Representative luminescence profiles of native HSE1 mutated and HSE-2 mutated Per2-Luc reporter after UV irradiation. Fold change of UV irradiated and no stimulated profiles are shown in the box-plot. *N* = 4, *: p<0.05, two-tailed t-tests.

Importantly, the circadian profile of HSE2 mutated Per2-Luc showed an arrhythmic pattern, indicating that HSE2 is indispensable for the UV-triggered clock synchronization (**Figure 2-13**). With Dex treatment, HSE-mutagenesis introduced reporters showed circadian rhythmic profiles. I further validated the origin of the acute surge using reporters originated from HSE sequences in Per2-Luc (minimal Per2HSE reporters), which luciferase is fused to the downstream of a native or mutated HSE sequences of the *Per*2 promoter (**Figure 2-14**). I observed reduced activation in HSE2 mutated minimal Per2HSE reporter which was consistent with the impaired acute surge in the HSE2 mutated Per2-Luc.

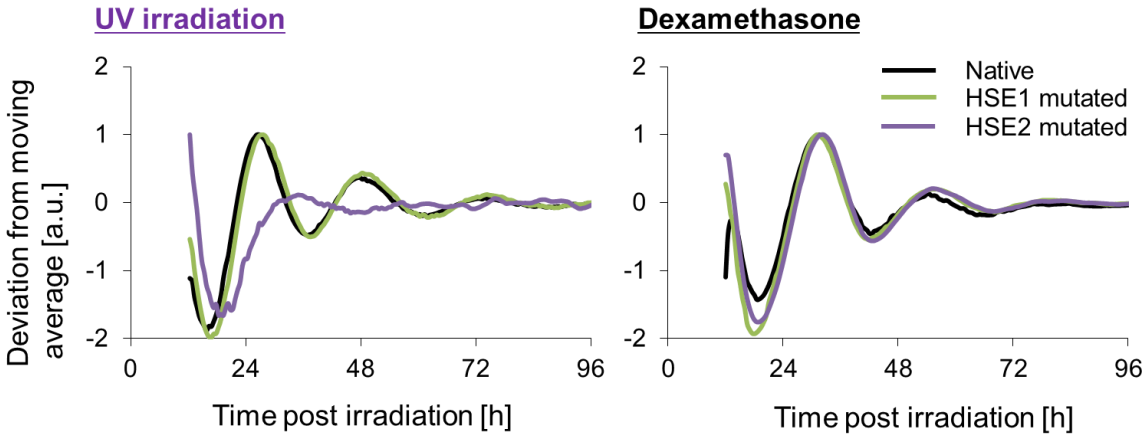

Figure 2-13. Detrended luminescence profiles of mutated Per2-Luc after UV irradiation.
Representative luminescence profiles of native HSE1 mutated and HSE-2 mutated Per2-Luc reporter after UV irradiation or Dex treatment.

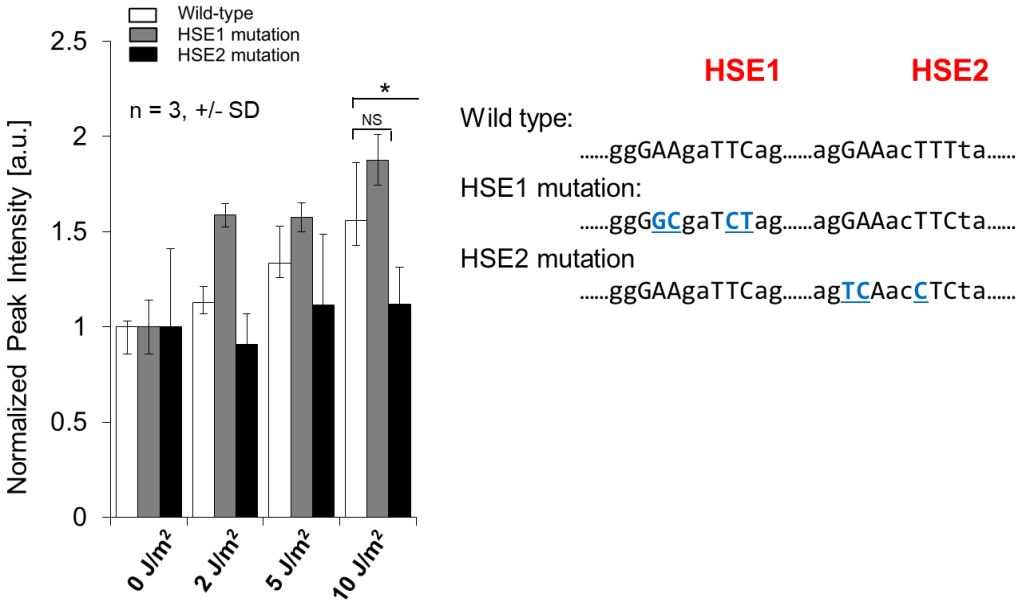

Figure 2-14. Luminescence profiles of minimal Per2HSE reporter after UV irradiation.
The normalized peak intensity of wild-type, HSE1 mutated and HSE-2 mutated minimal Per2HSE reporter after UV irradiation. HSE1 site and HSE2 site were mutated as shown in the figure.

To assess HSF1 binding to the HSE, ChIP assay was performed after UV irradiation (**Figure 2-15**). By the ChIP assay, the bound amount of transcription factors to the promoter can be evaluated. To assess rapid response of HSF1, I performed ChIP assay at 2 h after the UV irradiation. I found that HSF1 bound dominantly to HSE2, but not to HSE1, as also seen with HSF1 response to the heat-shock activation. These results demonstrated that UV irradiation induce HSF1 binding to the HSE2 site on *Per*2 promoter triggered by activation of HSR, thereby enhancing *Per*2 expression.

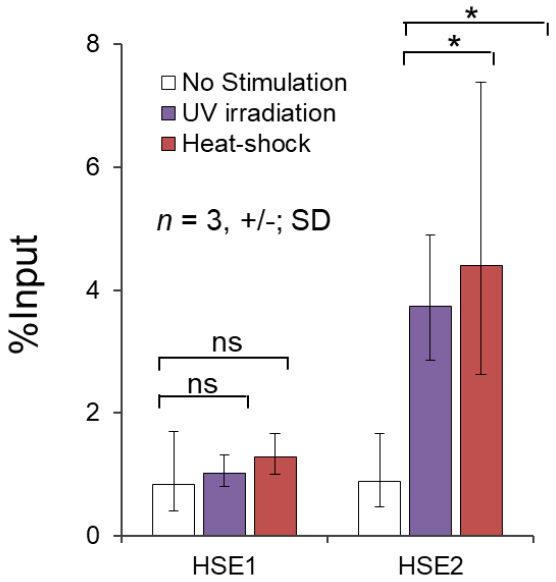

Figure 2-15. HSF1 binding to HSE2 on *Per*2 promoter.
ChIP assay against HSE1 and HSE2 on *Per*2 promoter using anti-HSF1 antibody. Immunoprecipitated DNA fragments were amplified using specific primers against HSE1 or HSE2. UV irradiation: 10 J/m^2, Heat-shock: 43°C 30 min. *N* = 4, +/-: SD. ns: not significant, *: p<0.05, two-tailed t-test.

2-3-2. p53 repress *Per*2 expression during UV-triggered clock synchronization

HSF1 is shown to be a trans-activator of *Per*2 post UV irradiation. However, single-cell HSE-SLR reporter assay suggested prolonged activation of HSF1, which HSF1 transcriptional activity profile continuously rose for more than 12 h post UV exposure. This observation does not completely match with Per2-Luc profile, which begins to fall within 8 h post UV exposure. These results implies the existence of a repression mechanism to modulate *Per*2 expression.

Recent studies demonstrate that p53 is a candidate mediator of circadian signaling by suppressing *Per*2 expression.[42] p53 is a responsible transcription factor of the anti-genotoxic response, and its transcriptional activity is increased by UV irradiation.[58] Hence, I investigated

whether p53 regulates resetting of the circadian clock by suppressing *Per*2 expression upon UV stimulation. First, I observed the response of Per2-Luc in wild-type and p53$^{-/-}$ MEFs. In wild-type MEFs, Per2-Luc initially elevated at 4-10 h post UV irradiation and then showed lowered luminescence. In p53$^{-/-}$ cells, altered Per2-Luc surge was observed at 8-16 h and maintained the elevation for more than one day post the irradiation (**Figure 2-16**). p53-mediated modulation role in *Per2* expression mechanism during UV-triggered clock synchronization may be the reason for longer lasting Per2-Luc surge. p53 is known to block BMAL1 binding to the E-box sequence adjacent to the p53 response-element (p53RE) of *Per2* promoter, thereby repressing *Per2* expression.[42] Accordingly, p53 potentially suppress *Per2* expression after ~10 h post UV irradiation in wild-type cells. Importantly, no significant circadian rhythm after UV irradiation was observed in p53$^{-/-}$ cells, whereas Dex treatment synchronized both cell types. Taken all, these results indicates p53 mediated pathway is pivotal in UV-triggered synchronization of circadian clock (**Figure 2-17**).

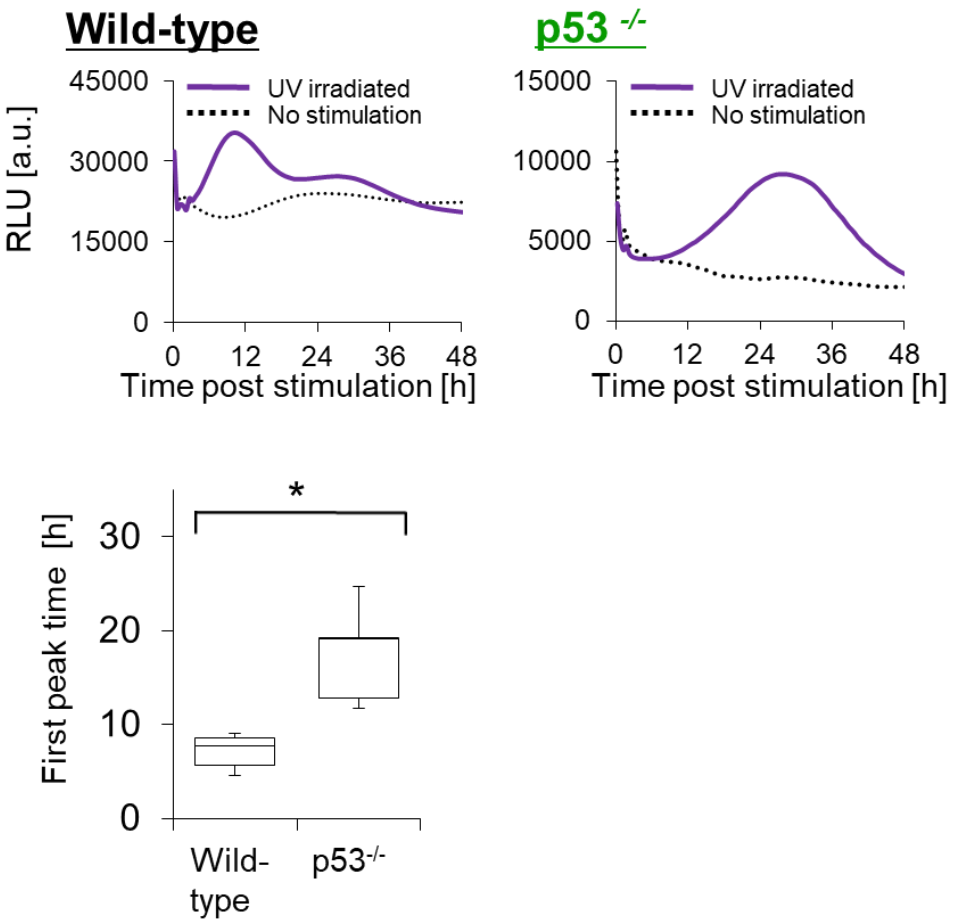

Figure 2-16. Per2-Luc initial surge in wild-type and p53$^{-/-}$ MEFs.
Per2-Luc profiles after UV irradiation (10 J/m^2) or no stimulation were observed in wild-type and p53$^{-/-}$ MEFs. Representative Per2-Luc profiles 0 to 24 h post irradiation is shown. Quantified duration of the first peak after the irradiation. *N* = 3, +/-: SD. ns: not significant, *: p<0.05, two-tailed t-test.

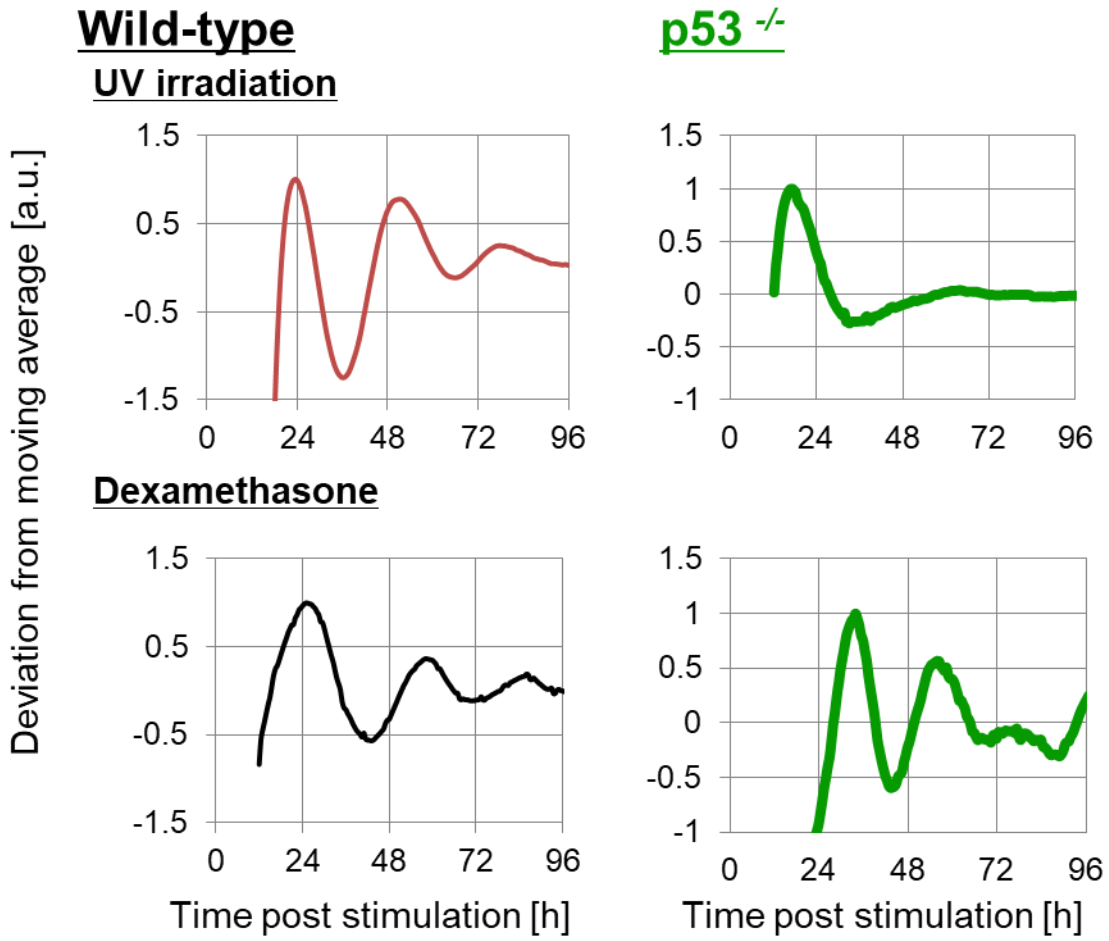

Figure 2-17. Per2-Luc oscillation in wild-type and p53$^{-/-}$ MEFs.
Per2-Luc profiles after UV irradiation (10 J/m^2) or Dex treatment (10 nM, 2 h) were observed in wild-type and p53$^{-/-}$ MEFs. Representative detrended Per2-Luc profiles post stimulations are shown.

Next, I conducted ChIP assay to determine whether p53 binds to the p53RE on *Per2* promoter after UV irradiation (**Figure 2-18**). ChIP assay was performed at 2 h post the irradiation to quantify the surge of p53 binding to respective elements. This assay revealed that p53 binds to p53RE adjacent to E-Box2, as well as to a positive control, p53RE in a known p53 target, *Mdm2* gene. However, no apparent binding was observed for E-Box5 adjacent to the HSE2 in *Per2* promoter. This supports the speculation that p53 suppress expression by binding to p53RE during UV-triggered clock synchronization. Considering these results, p53 is demonstrated to be another critical transcription factor that modulates *Per2* expression during UV-triggered clock resetting.

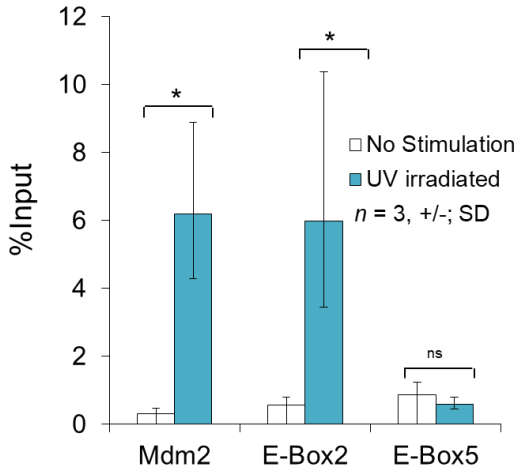

Figure 2-18. p53 binding to p53RE on *Per2* promoter.
ChIP assay against p53RE containing E-Box2 or E-Box5 on *Per2* promoter using anti-p53 antibody. Immunoprecipitated DNA fragments were amplified using specific primers against E-Box2, E-Box5 or p53RE on Mdm2 as a positive control. UV irradiation: 10 J/m^2. *N* = 3, +/-: SD. ns: not significant, *: p<0.05, two-tailed t-test.

2-3-3. HSF1 regulates p53 through their interaction during UV-triggered clock synchronization

These results indicate that at least two transcription factors, HSF1 and p53 are engaged in UV-triggered clock synchronization mechanism. Associations of HSF1 and p53 were reported to affect protection responses against proteotoxic and genotoxic stimulations.[31,59] Therefore, I hypothesized that HSF1 and p53 cooperatively regulate *Per2* expression during the clock synchronization to evoke protection responses against UV irradiation. To test the hypothesis, I utilized a real-time bioluminescence reporter assay, comprising of p53-response element-driven firefly luciferase (p53RE-Luc). I assessed p53 mediated transactivation by this reporter after UV irradiation in wild-type and HSF1$^{-/-}$ MEFs. In wild-type cells, p53RE-Luc activity elevated after UV irradiation within a circadian clock resetting dose. The increase in p53 mediated transcriptional regulation is considered to be involved in UV-triggered clock synchronization. In contrast, HSF1$^{-/-}$ MEFs cells showed substantially lowered p53RE-Luc surge after the UV irradiation, as compared with wild-type MEFs (**Figure 2-19**). These results demonstrate that HSF1 is pivotal for activation of p53 after UV irradiation. Conversely, p53$^{-/-}$ MEFs showed similar UV induced surge in HSE reporter to wild-type MEFs, suggesting that p53 does not

affect activation of HSF1 upon UV irradiation (**Figure 2-20**). These results show that HSF1 regulates p53 in a hierarchical manner, in which the presence of HSF1 is critical for p53 activation upon UV irradiation.

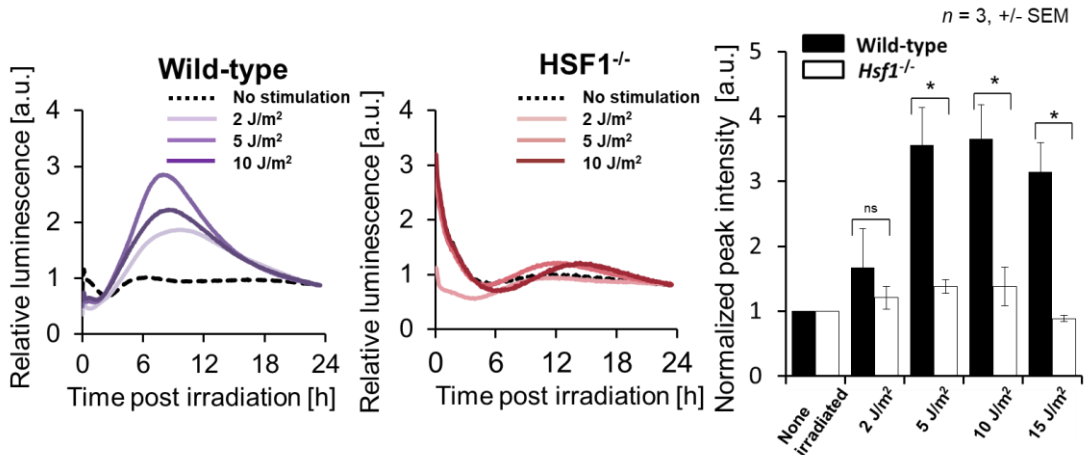

Figure 2-19. p53 transactivation in wild-type and HSF1$^{-/-}$ MEFs.
Reporter assay of p53 transactivation by the p53RE reporter was performed after UV irradiation in wild-type and HSF1$^{-/-}$ MEFs. Representative luminescence profiles are shown. Peak intensities were normalized to that of no stimulated sample. *N* = 3, +/-: SEM, ns: not significant, *: p<0.05, two-tailed t-test.

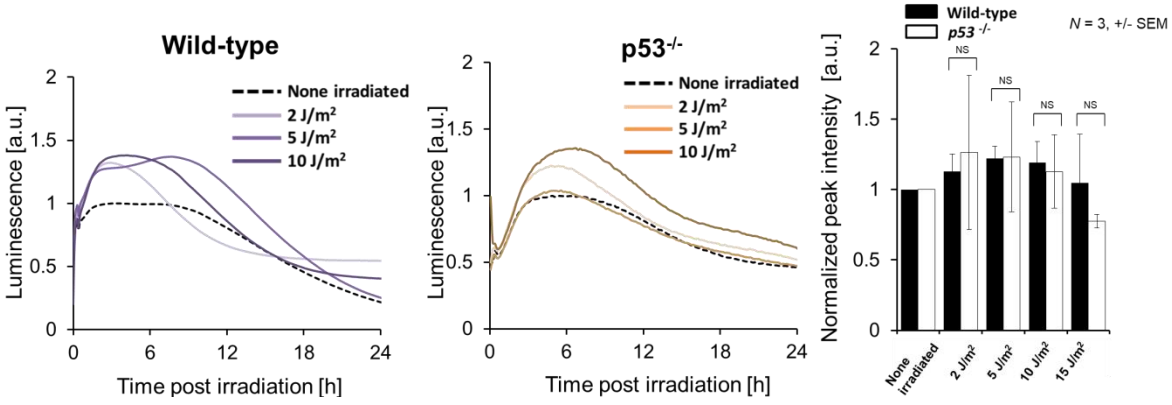

Figure 2-20. HSF1 transactivation in wild-type and p53$^{-/-}$ MEFs.
Reporter assay of HSF1 transactivation by HSE reporter was performed after UV irradiation in wild-type and p53$^{-/-}$ MEFs. Representative luminescence profiles are shown. Peak intensities were normalized to that of no stimulated sample. *N* = 3, +/-: SEM, ns: not significant, *: p<0.05, two-tailed t-test.

To examine whether direct HSF1–p53 binding serves for the molecular basis of HSF1–p53 interplay during UV triggered clock resetting, I conducted co-immunoprecipitation assays of HSF1 and p53 after UV stimulation (**Figure 2-21**). An acute increase in p53 bound HSF1 after UV irradiation was found in the immunoblot analysis for p53- co-immuno-precipitated HSF1. Additionally, p53 in HSF1-immunoprecipitates also showed a surge after the exposure, strongly suggesting UV irradiation-induced direct interactions of HSF1–p53. The temporal interaction

changes of HSF1–p53 were estimated by quantifying the band intensities of HSF1 and p53 immunoblotted bands after both co-immunoprecipitations. The result indicates that HSF1–p53 interaction increased at 2-4 h post UV irradiation.

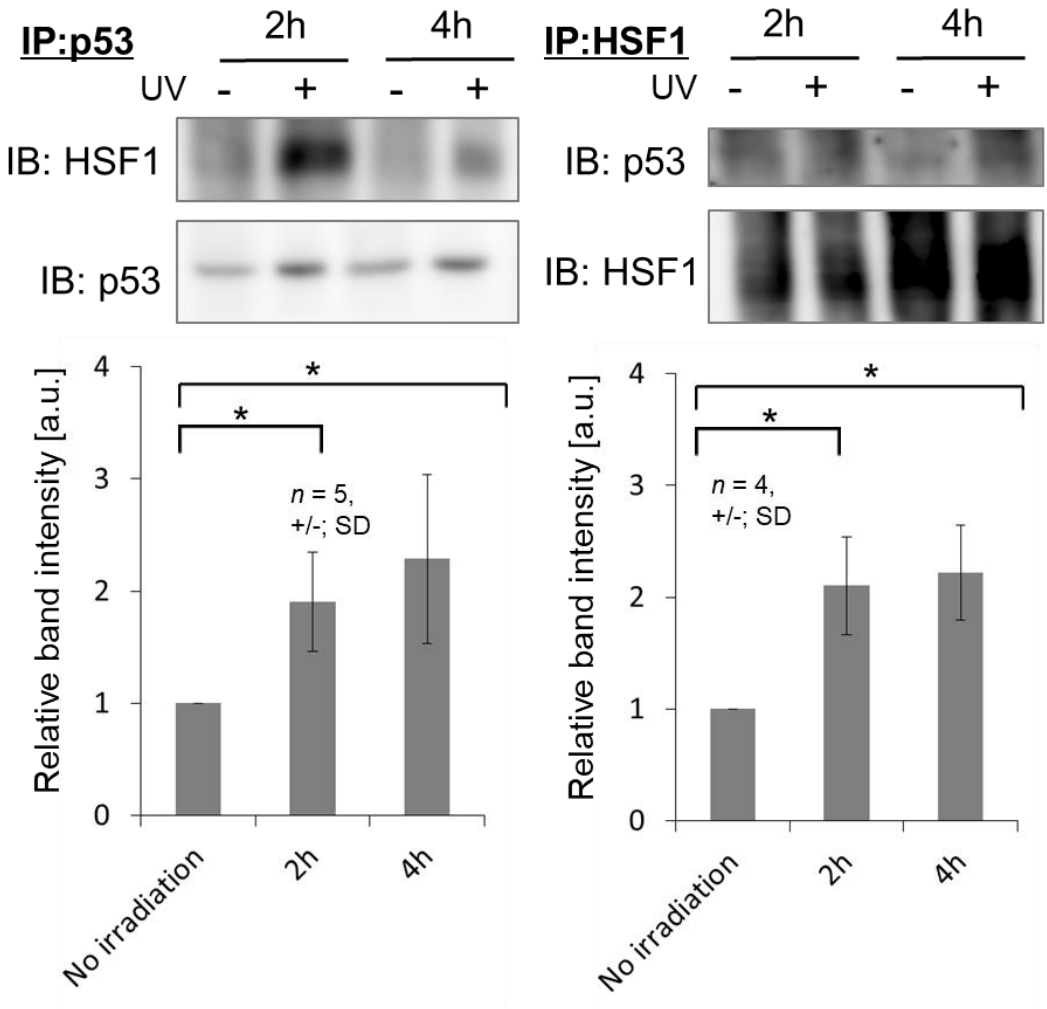

Figure 2-21. HSF1–p53 interactions after UV irradiation.
Co-immunoprecipitation assays to detect HSF1–p53 interactions. After UV irradiation, cells were lysed and immunoprecipitated with either anti-HSF1 or anti-p53 antibody. Immunoblot detections using the antibodies were performed to detect interacting complex. Number of replicates are written in the graph, +/-: SD, *: $p<0.05$, two-tailed t-test.

To reveal precise temporal kinetics of this interaction between HSF1 and p53 in living cells, a split-luciferase complementation assay was performed. In this assay, split fragments of luciferase are fused to HSF1 and p53 respectively. By using this technique, an interaction between HSF1 and p53 can be interpreted from bioluminescence from reconstituted luciferase. The luminescence profile demonstrates that HSF1–p53 interaction increased immediately after UV irradiation and began to decrease within 6 h post the irradiation. These results suggest

protein-protein interactions between HSF1 and p53 occur after UV irradiation, and these interactions are presumably a cue provoking regulation of p53 transcriptional activity by HSF1.

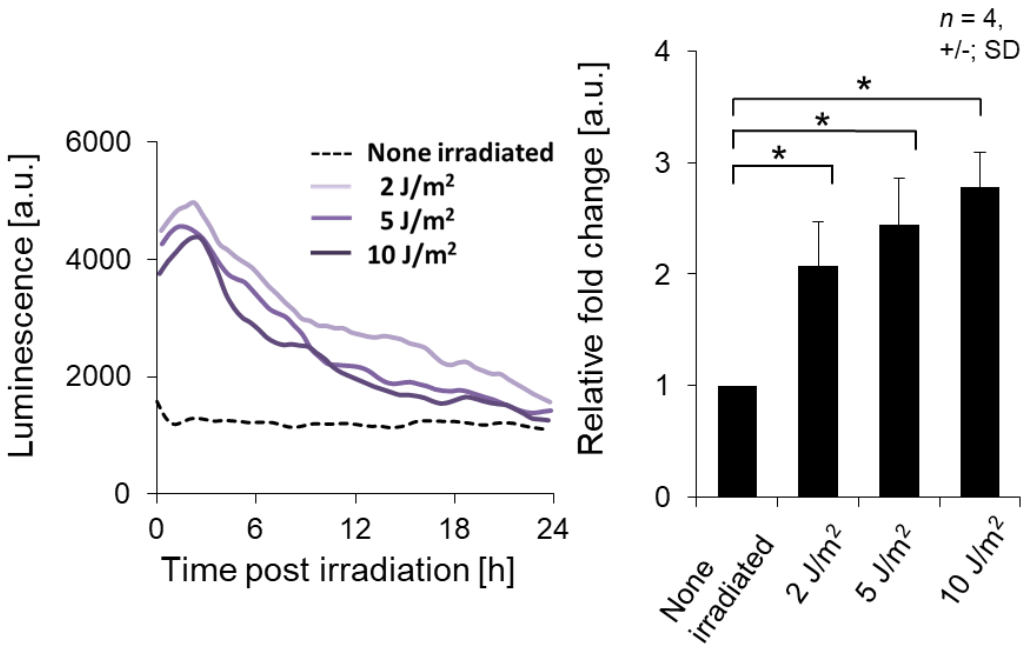

Figure 2-22. Real-time HSF1–p53 interaction reporter assays after UV irradiation. Split-luciferase complementation assays to detect HSF1–p53 interactions. Luminescence signal upon UV irradiation was measured with NIH3T3 cells expressing ELucN-HSF1 and ELucC-p53. *N* = 4, +/-: SD, *: p<0.05, two-tailed t-test.

2-3-4. BMAL1 regulates HSF1 and p53 through BMAL1‐HSF1 interaction during UV-triggered clock synchronization

The previous study revealed that an interaction between HSF1 and a circadian transcription factor BMAL1 is a critical step for the oxidative stress-induced clock synchronization.[24] Therefore, I expected that interplay between HSF1 and BMAL1 after UV irradiation is also an important feature of the clock synchronization process. Hence, I investigated the interplay between HSF1 and BMAL1 by co-immunoprecipitation assay (**Figure 2-23**). After UV irradiation, HSF1-bound fraction of BMAL1 increased in samples 2 and 4 h post irradiation. Consistent results were obtained from the blot for BMAL1-bound fraction of HSF1, suggesting HSF1 interacts with BMAL1 after the irradiation and the interaction prolongs at least 4 h during UV-triggered clock resetting. I then investigated whether HSF1–BMAL1 interaction affects their transcriptional activity. Since impaired UV triggered clock resetting response by HSF1 deficiency was suggested by arrhythmic Per2-Luc expression in HSF1$^{-/-}$ MEFs, I hypothesized that HSF1–BMAL1 interactions might mediate initial surge of Per2-Luc upon UV exposure.

Next, I conducted HSE-SLR reporter assay in BMAL1$^{-/-}$ MEFs cells to analyze the dependency of HSR to BMAL1. The result demonstrated that HSF1 activation upon UV stimulation is significantly impaired in BMAL1 deficient cells (**Figure 2-24A**). These results indicate that crosstalk between BMAL1 and HSF1 is induced at the early stage post UV irradiation, and BMAL1 is indispensable for UV-triggered activation of HSF1, as previously reported in the case by oxidative stress.[24] Notably, in BMAL1$^{-/-}$ MEFs cells, UV irradiation did not raise significant p53RE-Luc activation, which was observed in wild-type MEFs (**Figure 2-24B**). Taken that p53 response was also prohibited in HSF1$^{-/-}$ MEFs cells, impaired activation of p53RE-Luc in BMAL1$^{-/-}$ cells is likely to be a consequence of the lack of HSF1 activation due to BMAL1 deficiency. Taken together, circadian transcription factor BMAL1 likely to coordinates the adaptive responses of HSF1 and p53 against UV irradiation to synchronize cellular circadian clocks

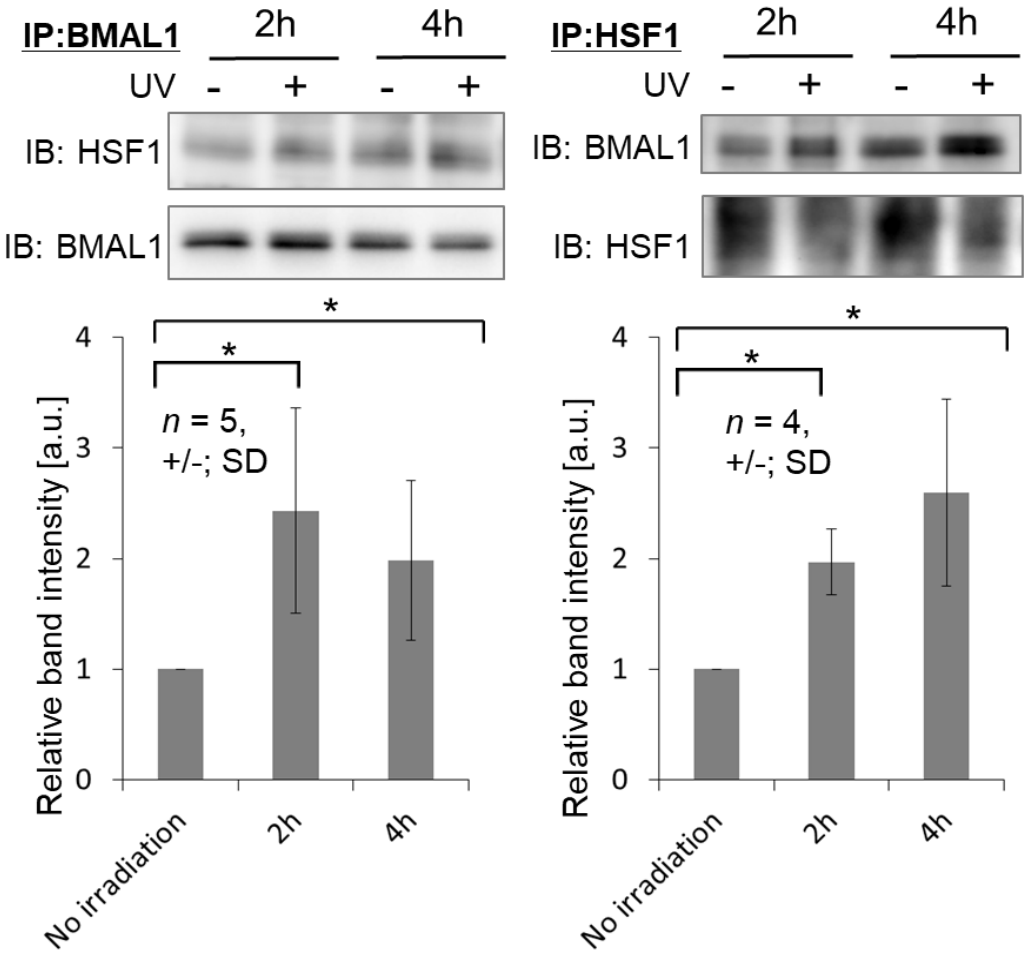

Figure 2-23. BMAL1–HSF1 interactions after UV irradiation.
Co-immunoprecipitation assays to detect BMAL1–HSF1 interactions. After UV irradiation, cells were lysed and immunoprecipitated with either anti-BMAL1 or anti-HSF1 antibody. Immunoblot detections using the antibodies were performed to detect interacting complex. Number of replicates are written in the graph, +/-: SD, *: $p<0.05$, two-tailed t-test.

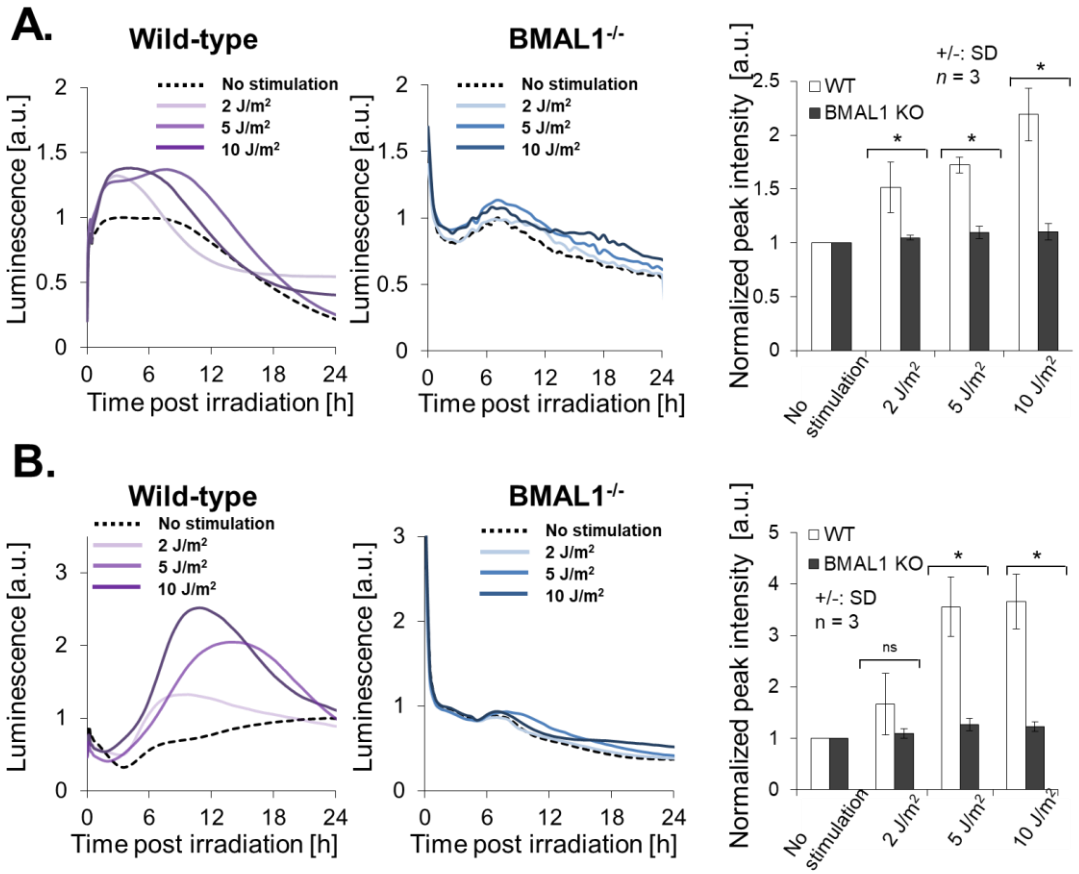

Figure 2-24. Effect of BMAL1 deficiency on HSF1 or p53 transactivation.
(A) Reporter assay of HSF1 transactivation by HSE reporter was performed after UV irradiation in wild-type and BMAL1$^{-/-}$ MEFs. Representative luminescence profiles are shown. Peak intensities were normalized to that of no stimulated sample. *N* = 3, +/-: SD, ns: no significant, *: p<0.05, two-tailed t-test. (B) Reporter assay of p53 transactivation by the p53RE reporter was performed after UV irradiation in wild-type and BMAL1$^{-/-}$ MEFs. Representative luminescence profiles are shown. Peak intensities were normalized to that of no stimulated sample. *N* = 3, +/-: SD, ns: not significant, *: p<0.05, two-tailed t-test.

2-3-5. Circadian time-dependent response of HSF1 and p53 to UV irradiation

Since the above findings imply that circadian trans-activator BMAL1 is a highly potential integrative regulator of UV induced transcription factors HSF1 and p53, I hypothesized that UV irradiation triggers activation of these transcription factors with circadian time-dependent manner. For this end, I characterized UV-triggered time-dependent phase shifting property of circadian clocks, as monitored with real-time Per2-Luc behaviors. NIH3T3 cells harboring Per2-Luc were synchronized with Dex treatment and then subjected to UV irradiation at the time from 24 to 48 h (defined as circadian time; CT 0 to 24 h) post-Dex treatment (**Figure 2-25A**). From the difference between the peak time of each Per2-Luc in UV-irradiated and

non-irradiated cells, I quantified UV-induced phase transition response of the clocks at each circadian time. By plotting the phase shifts over time on a phase response curve (PRC), I analyzed the time-dependent property of circadian clock synchronization by UV irradiation (**Figure 2-25B**). PRC diagram shows that UV irradiation induces a phase shift in a CT dependent manner. I also plotted transited phase on a phase transition curve (PTC) and found that UV induces synchronization of the circadian clock by a phase transition to a constant phase (CT = 0), indicating UV stimulation as a zero-type resetting synchronization factor (**Figure 2-25C**).[60]

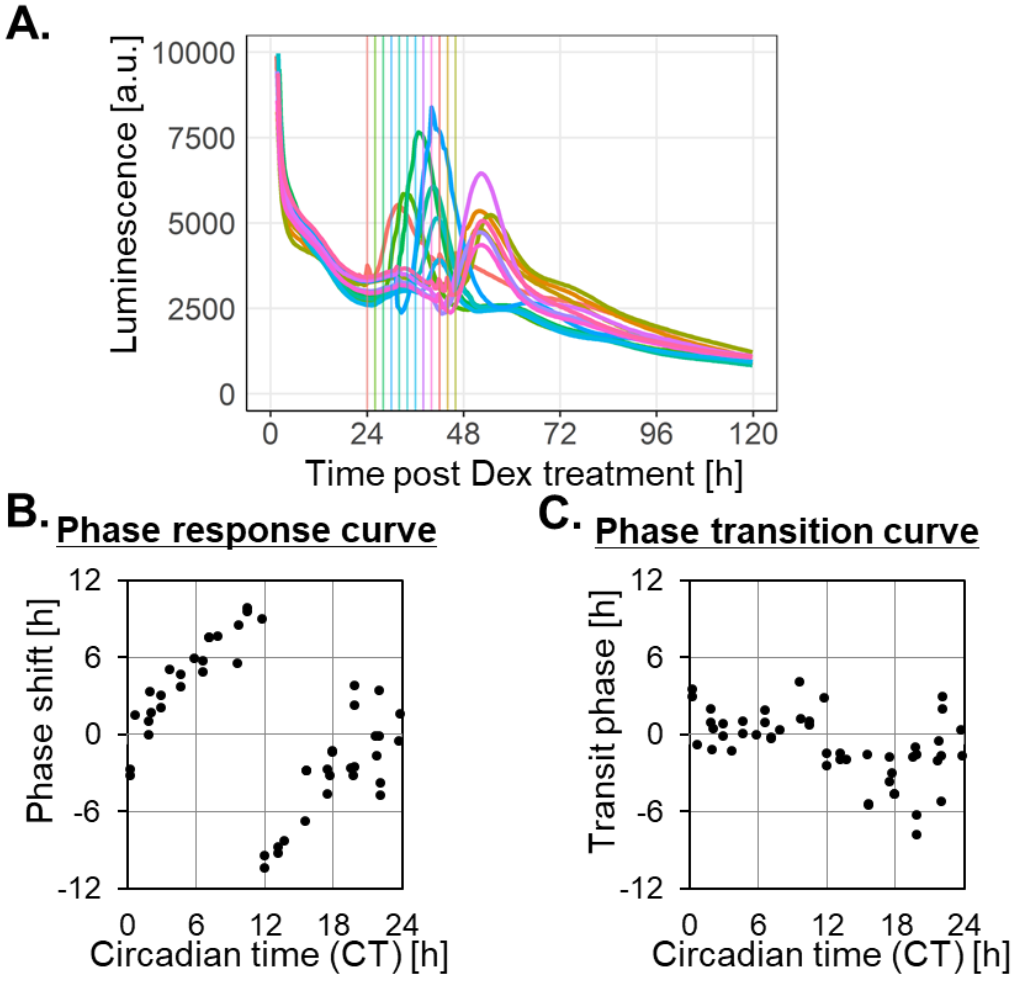

Figure 2-25. Circadian time-dependent response of Per2-Luc to UV irradiation. Circadian time-dependent analysis of UV irradiation-induced phase shift. NIH3T3 cell expressing Per2-Luc was treated with Dex for synchronization and UV irradiation was applied 24 to 48 h after Dex treatment. (A) Representative profiles of Per2-Luc after the irradiation. Irradiation time and corresponding luminescence profiles are color-coded with the same color. (B) The phase response curve of Per2-Luc after UV irradiation. Phase shift was calculated by the first peak time compared to no irradiated sample. Calculated phase shift was plotted against the time cells were irradiated. (C) Phase transition curve of Pe2-Luc after UV irradiation. Calculated phase shifts in (B) were used to derive the transit phase according to the time of irradiation.

synchronization, I further evaluated time-dependency of the activation of these two stress-responsive transcription factors, as monitored by real-time HSE-SLR and *Per*2 promoter originated p53RE-driven luciferase (p53RE/E-Box-Luc) reporter assays respectively. NIH3T3 cells expressing HSE-SLR or p53RE/E-Box-Luc were treated with Dex and irradiated with UV at CT 0-24 h. Luminescence profile before and after the UV irradiation at respective CTs was recorded for both reporters, and fold change in luminescence after the UV irradiation was quantified (**Figure 2-26A** and **B**). I observed time-dependent activation patterns of transcription factors HSF1 and p53, as demonstrated by the difference in the value of peak intensities, which corresponds to a degree of activation after the irradiation. Notably, the profile of the first peak intensity of HSE-SLR post UV synchronization showed the significant circadian time-dependent pattern as evaluated with ANOVA (p = 6.9x10^{-3}), with slightly higher intensity in CT 0-3 h compared to that in CT 4-7 h, and also in 12-15 h compared to that in 8-11 h. The highest intensity was in between CT 12-15 h to CT 16-19 h. For p53RE/E-Box-Luc reporters, peak intensity significantly fluctuated over CTs (F = 5.71, p = 6.0x10^{-4}, by ANOVA), exhibiting higher p53RE-Luc induction in CTs 0-3 h, 16-19 h and 20-23 h than that in CT 4-11 h. Taken together, these results indicate a circadian time-dependent response to UV stimulation of both HSF1 and p53 activity, presumably modulating *Per2* transcriptional regulation by UV irradiation.

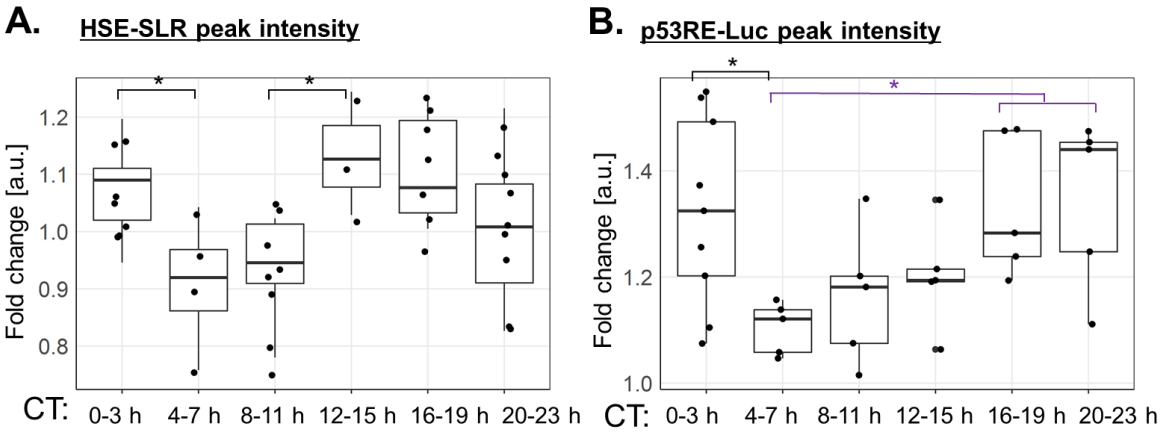

Figure 2-26. Circadian time-dependent response of HSF1 and p53 to UV irradiation. Circadian time-dependent analysis of UV irradiation-induced HSF1 and p53 transactivation. (A) NIH3T3 cell expressing HSE-SLR was treated with Dex for synchronization and UV irradiation was applied 24 to 48 h after Dex treatment (CT 0 to 24 h). Fold change of the first peak after the irradiation was quantified. Each profile was divided into groups determined by CTs and plotted as a box plot. At least 4 replicates for each group, *: p<0.05, two-tailed t-tests. (B) NIH3T3 cell expressing p53RE/E-Box-Luc was treated with Dex for synchronization and UV irradiation was applied 24 to 48 h after Dex treatment (CT 0 to 24 h). Fold change of the first peak after the irradiation was quantified. Each profile was divided into groups determined by CTs and plotted as a box plot. At least 5 replicates for each group, *: p<0.05, two-tailed t-tests.

analyzed CT-dependent binding of HSF1 and p53 transcription factors to *Per*2 promoter after UV irradiation. For this purpose, CT-dependent binding of HSF1 and p53 to *Per*2 promoter was evaluated by the ChIP assays. Dex-synchronized NIH3T3 cells were irradiated at the indicated CT and subjected to ChIP assays (**Figure 2-27**). I found a significant time dependency for the amount of HSF1 bound fraction to the DNA, where HSF1 binding was in significantly prominent level by UV irradiation at CT 0 and 6 h. In contrast, HSF1 binding was in substantially low level by the irradiation at CT 12 and 18 h. These data suggest that HSF1 mediated *Per*2 regulation upon UV irradiation was absent or weak at these CTs. On the other hand, significant p53 binding to *Per*2 promoter was observed by UV irradiation at all CTs with an almost constant level of the p53 binding upon UV exposure at all CTs. This result suggests that p53 mediated *Per*2 regulation constitutively active all over the day. Taken together, these results demonstrate that HSF1 and p53 bind to each respective consensus sequence on the *Per*2 promoter with CT-dependent manner to regulate *Per*2 expression.

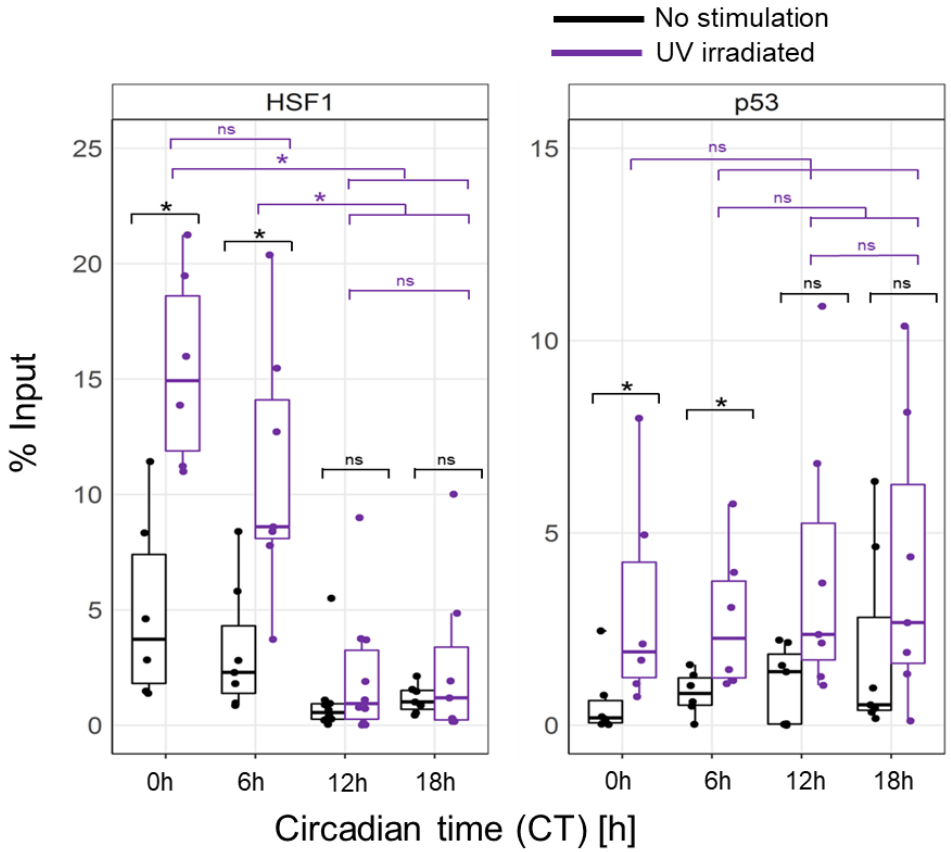

Figure 2-27. Circadian time-dependent binding of HSF1 and p53 to*Per*2 promoter
Circadian time-dependent analysis of UV irradiation-induced HSF1 and p53 binding to *Per*2 promoter. NIH3T3 cell was treated with Dex for synchronization and UV irradiation was applied 24 to 48 h after Dex treatment (CT 0 to 24 h). Immunoprecipitation using anti-HSF1 or anti-p53 was performed at each CT groups, and primers against HSE2 or p53RE on *Per*2 promoter was used to quantify the amount of immunoprecipitated DNA fragments. $N = 5$, ns: not significant, $p<0.05$, two-tailed t-test.

2-3-6. Transcriptomic analysis of UV induced signaling

From transcriptome data of MEF cells irradiated by UV, with similar dose to trigger clock synchronization taken from the NCBI database, I have found that together with the circadian clock system, a number of important stress-responsive pathways including apoptotic, cell-cycle regulation and oxidative stress as well as heat-shock response and DNA damage response pathways were inducted by the stimulation (**Figure 2-28**). Importantly, genes such as *Per*2, *Hsf*1, and *Trp*53 all increased after UV stimulation, supporting above-mentioned results. Notably, genes involved in heat-shock response increased earlier (44% of upregulated genes responded within 3 h post irradiation) than the genes assigned to DNA damage response and cell-cycle-related pathways (19% and 18% respectively), which support the findings that HSF1 modulates expression of p53 related genes. By comparing these transcriptome data with our previous microarray data from fibroblasts stimulated by ROS to trigger clock-synchronization,[24] I noticed that some of the transcripts belonging to these stress-responsive pathways increased in both UV and ROS stimulation. However, the majority of the transcripts were regulated with a characteristic pattern to respective stimulation (**Figure 2-29**), indicating that UV and ROS regulate genes associated to similar pathways at the global level, although differential regulation exists at an individual transcript level. Intriguingly, circadian-related genes, *Dbp*, and *Timeless* commonly increased at 3-6 h post UV irradiation and 4 h post ROS exposure (**Figure 2-30**). *Timeless* is known to be involved in the DNA responsive circadian organization,[61] indicating that acute and long-lasting increase of *Timeless* is potential a regulatory event in cellular stress adaptation through the circadian clock. I also found increase in the expression of p53 related genes such as *Gadd45a* and *Trp53*, a heat-shock response gene *Ccs*, an anti-oxidant gene *Mt1* and *Sod2*, and apoptosis/inflammatory–related genes such as *Akt1*, *Bcl2l11*, *Casp3* and *Nfkbib*, implying that UV and ROS stress exposure booted common pathways via expression of specific genes, which likely contribute to the common adaptive responses to the cellular stresses. Importantly, prior to them, HSF1-regulated genes such as *Hsp70* and *Hspb1*, and the majority of the E-box-controlled genes such as *Per1/2* and *Cry1* acutely surged within 3 h post UV stimulation, supporting our notion that clock and HSR pathways synergistically evoke adaptation to the cellular stresses. These UV induced gene expression profiles of the circadian and stress-related pathways lead to elucidation of a network structure of the adaptive responses, where UV irradiation triggers activation of transcription factors HSF1 and p53, through synergistic interplay with the circadian system, subsequently driving cellular adaptive protection system via DNA damage, anti-oxidant, cell-cycle related and apoptotic pathways (**Figure 2-31**).

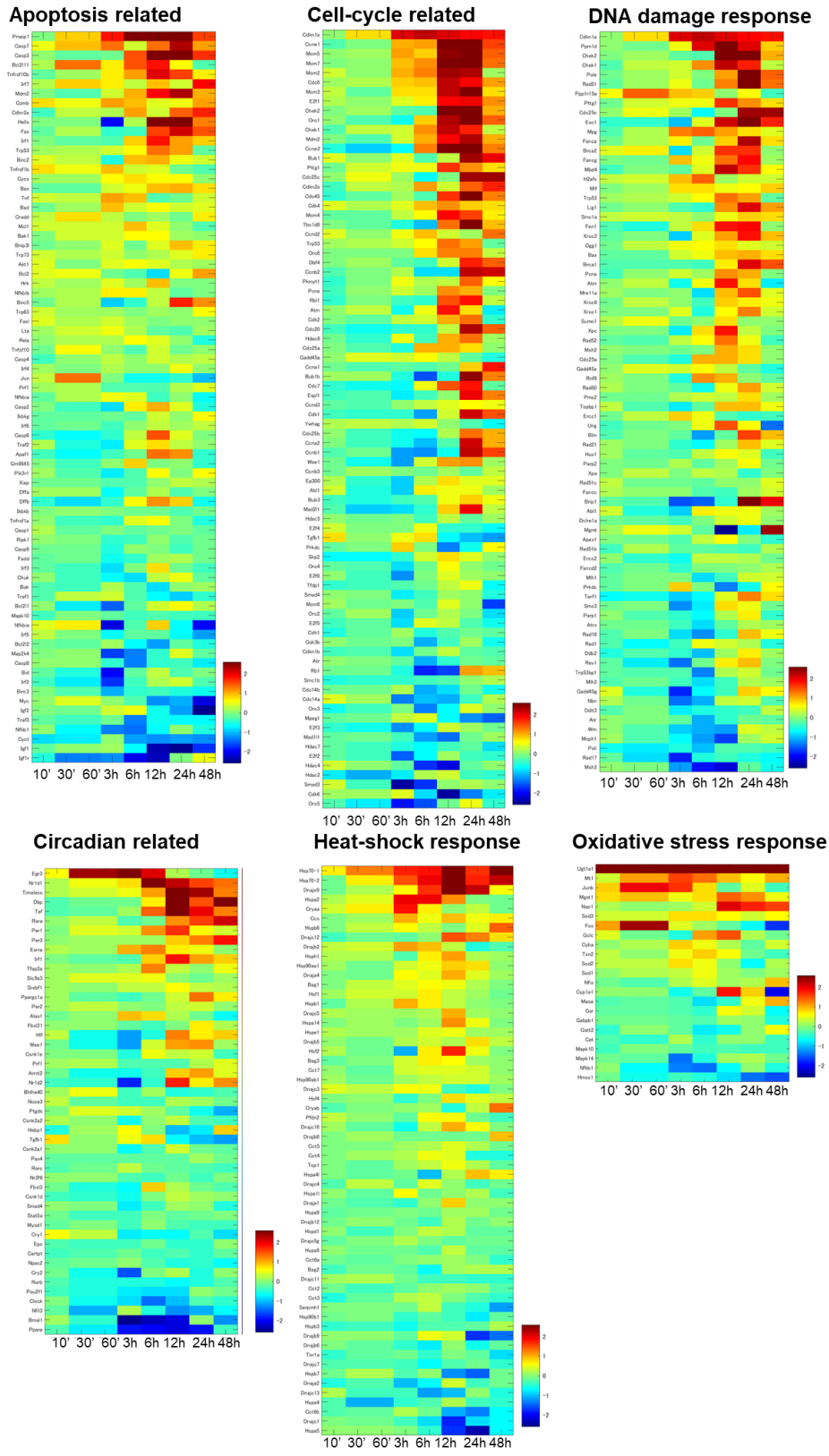

Figure 2-28. Global assessment of UV induced gene expressions.
Gene expression profiles of apoptosis, cell cycle, DNA damage response, circadian, heat-shock response, and oxidative stress were extracted and its expression change over time are color coded. Data were obtained from NCBI GEO (GSE50930).

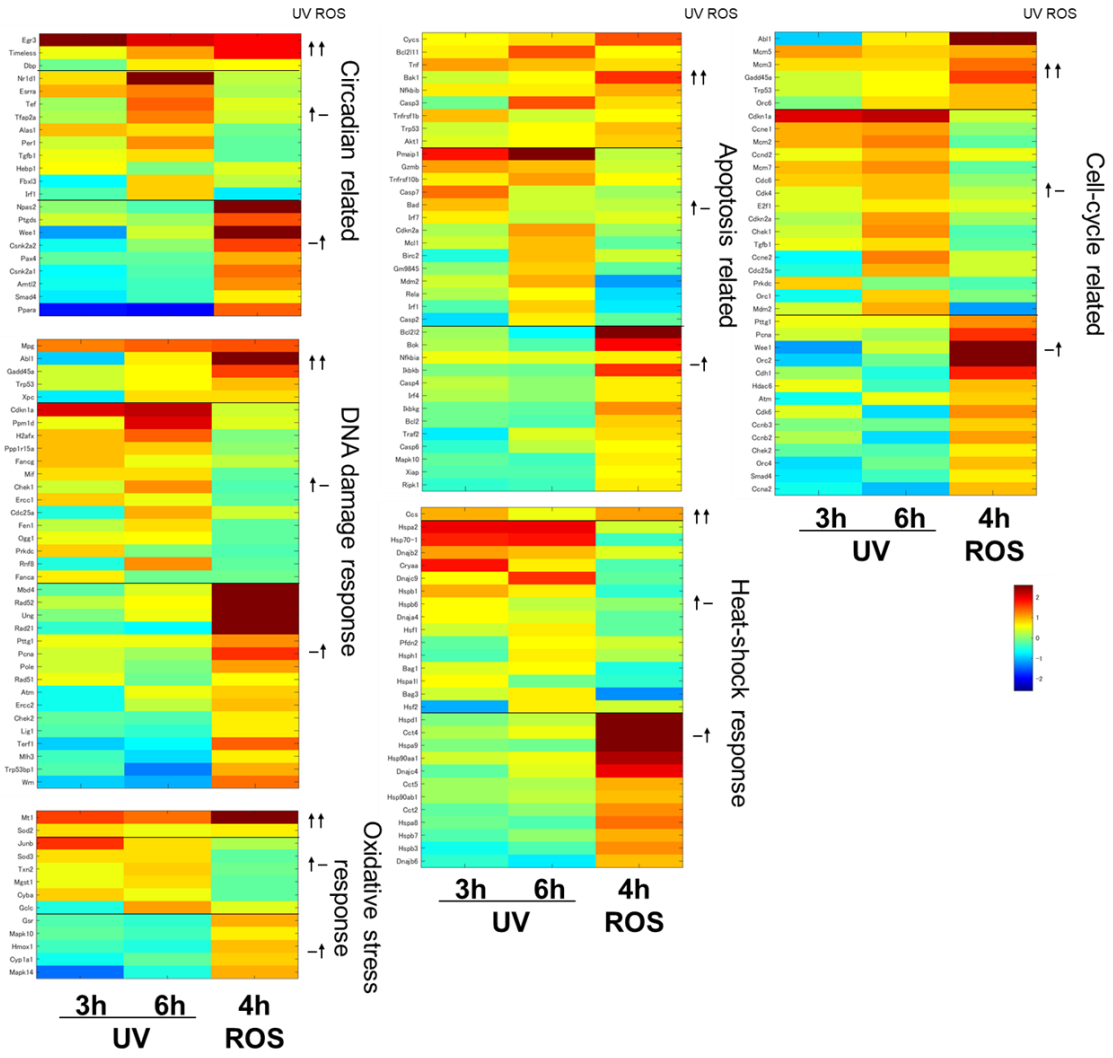

Figure 2-29. Comparison of UV induced and ROS induced gene expressions.
Gene expression profiles of apoptosis, cell cycle, DNA damage response, circadian, heat-shock response, and oxidative stress, which increased at least 1.5 times for at least in one of the stimulation were extracted and its expression change over time are color coded. Arrow indicates induction. Data were obtained from NCBI GEO (UV: GSE50930, ROS: GSE47955).

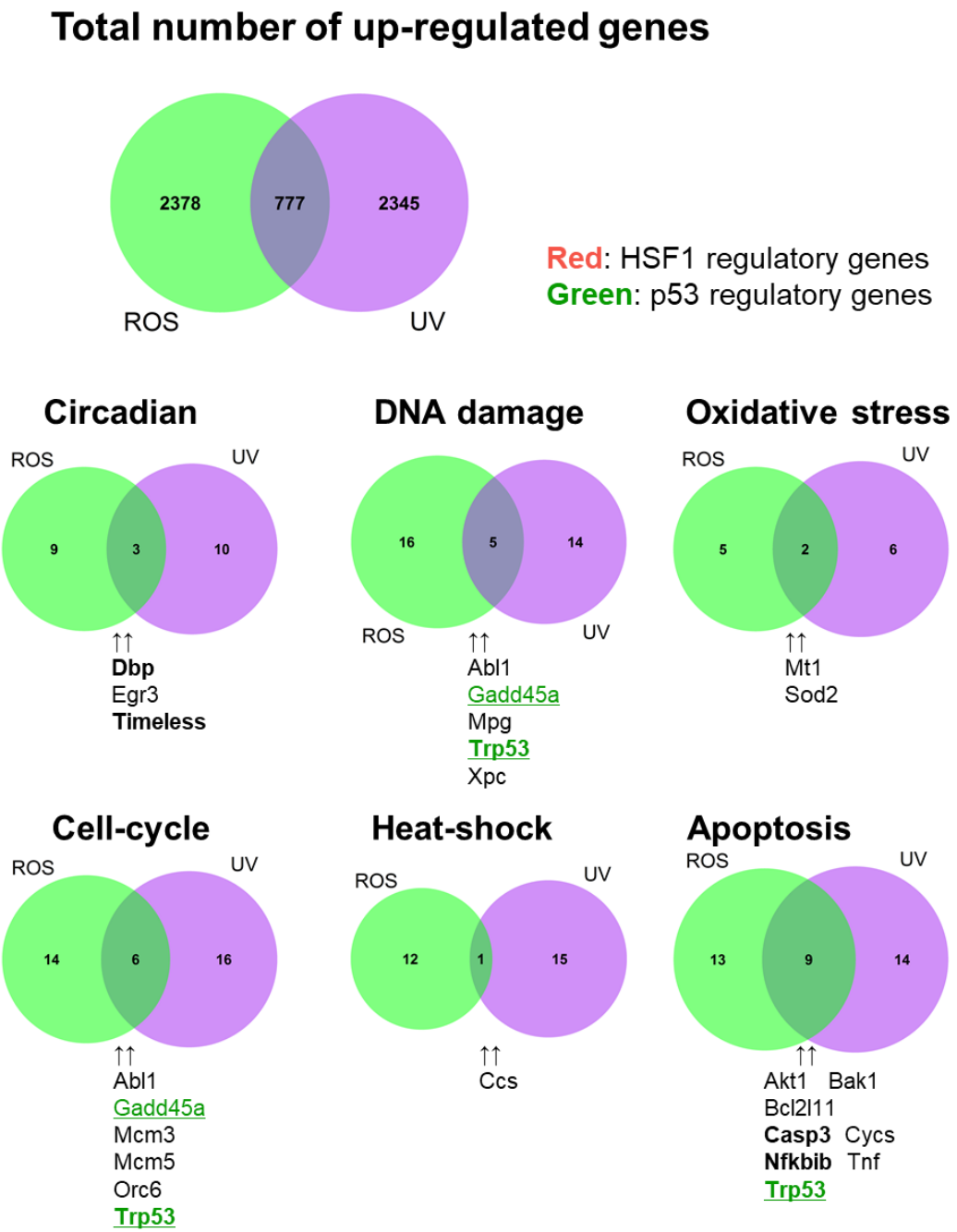

Figure 2-30. Commonly inducted genes among UV and ROS stimulations.
Gene that increased at least 1.5 times fold were extracted for each stimulation. Venn diagram represents genes that changed specifically to either UV or ROS stimulation or changed in both stimulations. Names of genes that changed in both stimulations are shown. Bold names indicate genes that are considered important for this study. Red names indicate HSF1 regulatory genes and green names indicate p53 regulatory genes.

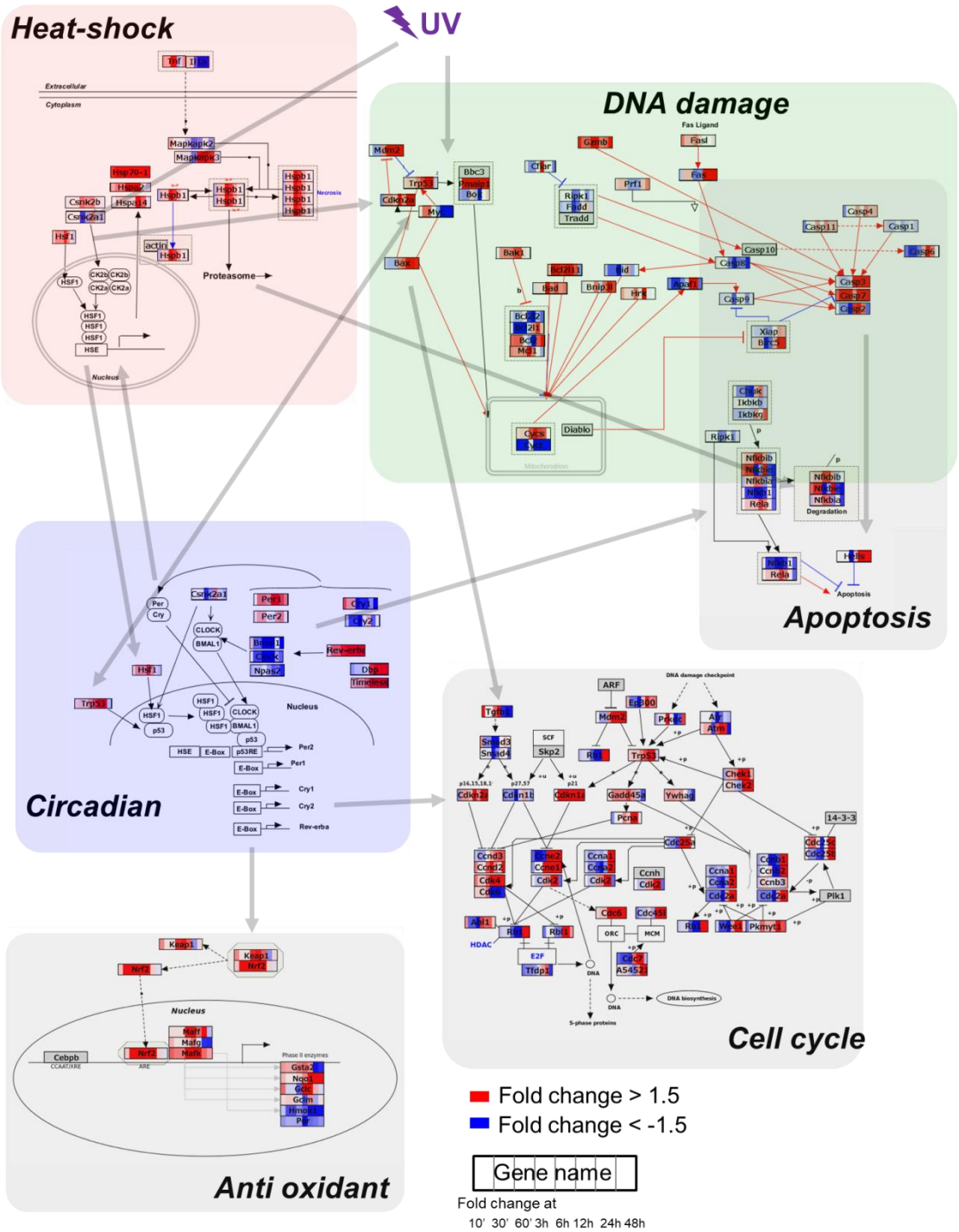

Figure 2-31. Pathway map for UV regulated gene expression.
Gene expression profiles for UV stimulations were mapped to prior knowledge of stress-responsive signaling pathways using PathVisio software using WikiPathway as a source of the maps. Gene expression profiles for apoptosis-related, cell-cycle related, DNA damage response, circadian clock, heat-shock response, and oxidative stress systems were mapped. The direction of an arrow indicates regulatory relationships between pathways.

2-4. Discussion

In this study, I investigated interplays between the circadian timing system and stress response pathways during clock synchronization in response to UV irradiation, based on our previously proposed notion that molecular networks among circadian clock and adaptive protection pathways such as HSR have vital roles in the stress-responsive clock synchronization to evoke protective responses.[24,25] Supporting our notion, central transcription factor HSF1 of the HSR pathway is identified as a circadian-recruited DNA binding protein in the liver,[27] and it is now widely known that body temperature change and heat-shock stimuli synchronize mammalian peripheral clocks via HSF1.[25,62,63] Several pieces of evidence demonstrate a correlation between molecular clocks and p53, an anti-oncogene indispensable for anti-genotoxic pathway. One example is that p53 activity is controlled by BMAL1 in the pancreas cancer.[64] In addition, p53 negatively regulates a clock gene *Per*2 expression,[42] This evidence imply that molecular clock responds to the genotoxic stress to reset its phases, and simultaneously regulates genotoxic stress response pathways. According to previous work, the time-dependent phase shift of the clocks is observed in response to the critical cellular stress such as gamma-ray irradiation,[65,66] indicating that clock system is reset in response to such stress with circadian time-dependent manner. This may be due to differentially regulated stress- responsive molecular networks at each circadian time. Therefore, I hypothesized that stress responses occur with the circadian time-dependent manner and the molecular basis for the time-dependent stress responses probably originates from molecular processes during clock synchronization at each circadian time. As the pivotal molecular process, I here focused on interplays among BMAL1, HSF1, and p53 during and after UV-triggered clock synchronization and investigated it especially in their circadian time-dependent context.

To test this concept, I first analyzed how stress-responsive transcription factors respond to UV irradiation, and focused on their interactions post stress exposure. I first analyzed clock-resetting responses after UV irradiation as manifested by Per2-Luc surge post the stimulation. According to previous work that analyzes the differential effect of UV irradiation over circadian time in a mice model, DNA repair is higher in the afternoon, when elevated *Cry*1/2 are observed.[28] Another paper describes the increased level of protein amount of *Cry*1 and *Per*2 was observed after γ-ray irradiation, and mutation of *Per*2 reduces expression of genotoxic resistance genes, indicating *Per*2 may play a key role in the protection from DNA damage.[29] This supports our data showing that transcriptional upregulation of *Per*2 is considered to be a marker for the occurrence of cellular protection towards UV induced stresses. Using

Per2-Luc as an indicator of circadian rhythm, I have shown that HSF1 (**Figure 2-7**) and p53 (**Figure 2-17**) is necessary for UV-triggered clock synchronization. Supporting this, the components of their corresponding pathways are upregulated after UV irradiation, probably via direct trans-activation by HSF1 and p53, as observed with luminescent reporter assays (**Figure 2-20**). Impairment of UV-triggered clock synchronization by a deficiency of HSF1 demonstrates that HSF1 is indispensable for the synchronization. As previously reported, the pivotal role of HSF1 is common to clock synchronization by heat-shock and ROS induced cellular stress,[24,25] suggesting that HSF1 is a general mediator for cellular stress induced clock synchronization. Deficiency of p53 results in impairment of UV-triggered clock synchronization and also Per2-Luc surge after UV exposure, indicating that p53 may function along with BMAL1 and HSF1 mediated transcriptional regulation. Taken together, p53 mediates the clock-synchronizing signal with partially HSF1-dependent manner, as the presence of HSF1 is necessary for p53 trans-activation, which suggests a hierarchal structure that HSF1 is up-regulator of p53 after UV irradiation. Moreover, activation of both HSF1 and p53 are largely suppressed in cells lacking circadian transcription factor BMAL1, demonstrating that BMAL1 is indispensable for the functions of HSF1 and p53 during UV-triggered clock synchronization, and strongly suggesting that BMAL1 coordinates cellular protection response against UV-induced stress (**Figure 2-24**). Considering all of the above, I have elucidated a hierarchal network of transcription factors comprising of integrative regulator BMAL1, BMAL1-regulated heat-shock responsive HSF1 and HSF1-dependently activated p53. Our findings highlight a concept that stress responsive cellular protection systems are booted during the resetting of circadian clocks.

Daily time-dependent molecular and physiological responses are based on the coordination by the circadian clock system. I have found that both HSF1 and p53 are activated in a circadian time-dependent manner, with distinct patterns. The timing of their peaks in the activities after UV exposure differ according to the circadian time (CT) as defined by the time post Dex treatment, and peak intensities of both reporters show an oscillation pattern reaching the peak at CT: 16-19h and the trough at CT: 4-7h (**Figure 2-26**). These results indicate circadian time-dependent and differential action of HSF1 and p53 in response to UV-irradiation. As expected, I found daily fluctuation in HSF1 and p53 binding to *Per*2 promoter detected by time-dependent ChIP assays, with predominant binding to the promoter in CT 0 and 6 h (**Figure 2-27**).

Since the activation pattern of HSF1 and p53 shows time-dependency and decreased activities in BMAL1-deficient cells post UV exposure, BMAL1 might control HSF1 and p53 activities during clock synchronization. Indeed, BMAL1 is considered to be a regulator of p53 pathway that controls transcriptional activity of p53.[45] Moreover, binding of HSF1 and p53 to

*Per*2 promoter with similar timing (**Figure 2-7**) and reduced response of p53RE-Luc in HSF1-deficient cells (**Figure 2-19**) post UV exposure suggests that HSF1, as well as BMAL1, simultaneously controls transcriptional activation of p53 upon stimulation. These results suggest that time-dependent binding of HSF1 and p53 to *Per*2 promoter is likely to be a major cause for the time-dependent response of Per2-Luc after UV irradiation. Taken together, our results suggest a network of interactions between circadian clock system and stress response pathways, where BMAL1 acts as a master organizer in BMAL1-HSF1-p53 -mediated molecular network for resetting clocks to boot adaptive protection responses against the cellular stress, represented by UV exposure.

The circadian clock is hypothesized to be an escape from DNA replication in the cell cycle by predicting when DNA damaging stimulation occurs during the day and night cycle.[1] Although more intensive analysis of the relationships between circadian clock system and clock-timekeeping phenomena such as cell division cycle and cellular metabolism is necessary, I believe our model highlighting interactive connections among circadian clock system and stress response pathways during clock synchronization post the stress exposure would provide a novel insight into the concept that circadian system boot up stress responsive cellular protection systems during stress-triggered resetting of circadian clock, controlling stress response pathways to adopt toward the vital environmental changes.

2-5. Conclusion

In this chapter, I described a perturbation of the cellular system by UV irradiation and analyzed the effect on the circadian clock system. In this study, I used UV irradiation as an optical perturbation system. For the analysis, I employed reporter gene assay system, where regulation of transcription is able to be monitored by the optical signal. The combination with standard biochemical assays leads to the elucidation of molecular mechanisms underlying synchronization of the circadian clock by UV irradiation. Because circadian clock synchronization is a time-dependent process, temporal analysis on the transcriptional regulations was conducted owing to the character of optical perturbation system. I succeeded in demonstrating that circadian time-dependent transcriptional activity of HSF1 and p53 cause time-dependent circadian clock synchronization as manifested with monitoring of *Per2* expression. Moreover, by observing global gene expression pattern and comparing it with previous studies, commonly inducted signaling pathways with other stress-inducing stimulations were identified, highlighting the use of transcriptomic analysis as a powerful method for the identification of signaling pathways.

As shown in this chapter, a combination of analyzing specific gene abundance or transcription factor activation by the reporter assay and global analysis of the transcriptomic landscape would complement each other for revealing unknown molecular mechanisms. In addition, optical perturbation succeeded in unveiling the time-dependent transcriptional regulation of *Per2* expression which results in synchronization of the circadian clock. Taken together, these results demonstrate that optical perturbation system serves as a platform for revealing the causative relationships on the time-dependent transcriptional regulation.

References

1. Sahar, S. & Sassone-Corsi, P. Metabolism and cancer: the circadian clock connection. *Nat. Rev. Cancer* **9**, 886–896 (2009).
2. Schibler, U. & Sassone-Corsi, P. A web of circadian pacemakers. *Cell* **111**, 919–922 (2002).
3. Takahashi, J. S. Transcriptional architecture of the mammalian circadian clock. *Nat. Rev. Genet.* **18**, 164–179 (2016).
4. Schibler, U. & Sassone-Corsi, P. A Web of Circadian Pacemakers. *Cell* **111**, 919–922 (2002).
5. Kondo, T. *et al.* Circadian clock mutants of cyanobacteria. *Science* **266**, 1233–1236 (1994).
6. Ishiura, M. *et al.* Expression of a Gene Cluster kaiABC as a Circadian Feedback Process in Cyanobacteria. *Science* **281**, 1519–1523 (1998).
7. Pittendrigh, C. S., Bruce, V. G., Rosensweig, N. S. & Rubin, M. L. Growth Patterns in Neurospora: A Biological Clock in Neurospora. *Nature* **184**, 169–170 (1959).
8. Konopka, R. J. & Benzer, S. Clock Mutants of Drosophila melanogaster. *Proc. Natl. Acad. Sci.* **68**, 2112–2116 (1971).
9. Vitaterna, M. H. *et al.* Mutagenesis and mapping of a mouse gene, Clock, essential for circadian behavior. *Science* **264**, 719–725 (1994).
10. Boivin, D. B., Duffy, J. F., Kronauer, R. E. & Czeisler, C. A. Dose-response relationships for resetting of human circadian clock by light. *Nature* **379**, 540–542 (1996).
11. Panda, S., Hogenesch, J. B. & Kay, S. A. Circadian rhythms from flies to human. *Nature* **417**, 329–335 (2002).
12. Yamazaki, S. *et al.* Resetting Central and Peripheral Circadian Oscillators in Transgenic Rats. *Science* **288**, 682–685 (2000).
13. Dibner, C., Schibler, U. & Albrecht, U. The Mammalian Circadian Timing System: Organization and Coordination of Central and Peripheral Clocks. *Annu. Rev. Physiol.* **72**, 517–549 (2010).
14. Stephan, F. K. & Zucker, I. Circadian Rhythms in Drinking Behavior and Locomotor Activity of Rats Are Eliminated by Hypothalamic Lesions. *Proc. Natl. Acad. Sci.* **69**, 1583–1586 (1972).
15. Welsh, D. K., Logothetis, D. E., Meister, M. & Reppert, S. M. Individual neurons dissociated from rat suprachiasmatic nucleus express independently phased circadian firing rhythms. *Neuron* **14**, 697–706 (1995).
16. Berson, D. M., Dunn, F. A. & Takao, M. Phototransduction by Retinal Ganglion Cells That Set the Circadian Clock. *Science* **295**, 1070–1073 (2002).
17. Nagoshi, E. *et al.* Circadian Gene Expression in Individual Fibroblasts: Cell-Autonomous and Self-Sustained Oscillators Pass Time to Daughter Cells. *Cell* **119**, 693–705 (2004).
18. Balsalobre, A., Damiola, F. & Schibler, U. A Serum Shock Induces Circadian Gene Expression in Mammalian Tissue Culture Cells. *Cell* **93**, 929–937 (1998).
19. Yamaguchi, S. *et al.* Synchronization of Cellular Clocks in the Suprachiasmatic Nucleus. *Science* **302**, 1408–1412 (2003).
20. Buhr, E. D., Yoo, S.-H. & Takahashi, J. S. Temperature as a Universal Resetting Cue for Mammalian Circadian Oscillators. *Science* **330**, 379–385 (2010).
21. Ko, C. H. & Takahashi, J. S. Molecular components of the mammalian circadian clock. *Hum. Mol. Genet.* **15**, 271–277 (2006).
22. Dibner, C. *et al.* Circadian gene expression is resilient to large fluctuations in overall transcription rates. *EMBO J.* **28262**, 123–134 (2009).
23. Tamaru, T. & Ikeda, M. Circadian adaptation to cell injury stresses: a crucial interplay of BMAL1 and HSF1. *J. Physiol. Sci.* **66**, 303–306 (2016).

24. Tamaru, T. *et al.* ROS stress resets circadian clocks to coordinate pro-survival signals. *PLoS ONE* **8**, 1–16 (2013).
25. Tamaru, T. *et al.* Synchronization of circadian Per2 rhythms and HSF1-BMAL1:clock interaction in mouse fibroblasts after Short-Term heat shock pulse. *PLoS ONE* **6**, 1–7 (2011).
26. Fu, L., Pelicano, H., Liu, J., Huang, P. & Lee, C. C. The circadian gene Period2 plays an important role in tumor suppression and DNA damage response in vivo. *Cell* **111**, 41–50 (2002).
27. Reinke, H. *et al.* Differential display of DNA-binding proteins reveals heat-shock factor 1 as a circadian transcription factor. *Genes Dev.* **22**, 331–345 (2008).
28. Papp, S. J. *et al.* DNA damage shifts circadian clock time via hausp-dependent cry1 stabilization. *eLife* **2015**, 1–19 (2015).
29. Gotoh, T., Vila-Caballer, M., Liu, J., Schiffhauer, S. & Finkielstein, C. V. Association of the circadian factor Period 2 to p53 influences p53's function in DNA-damage signaling. *Mol. Biol. Cell* **26**, 359–372 (2015).
30. Min, J.-N., Huang, L., Zimonjic, D. B., Moskophidis, D. & Mivechi, N. F. Selective suppression of lymphomas by functional loss of Hsf1 in a p53-deficient mouse model for spontaneous tumors. *Oncogene* **26**, 5086–5097 (2007).
31. Logan, I. R. *et al.* Heat shock factor-1 modulates p53 activity in the transcriptional response to DNA damage. *Nucleic Acids Res.* **37**, 2962–2973 (2009).
32. Morimoto, R. I. Regulation of the heat shock transcriptional response: cross talk between a family of heat shock factors, molecular chaperones, and negative regulators. *Genes Dev.* **12**, 3788–3796 (1998).
33. Westerheide, S. D., Anckar, J., Stevens, S. M., Sistonen, L. & Morimoto, R. I. Stress-Inducible Regulation of Heat Shock Factor 1 by the Deacetylase SIRT1. *Science* **323**, 1063–1066 (2009).
34. Åkerfelt, M., Morimoto, R. I. & Sistonen, L. Heat shock factors: integrators of cell stress, development and lifespan. *Nat. Rev. Mol. Cell Biol.* **11**, 545–555 (2010).
35. Vihervaara, A. & Sistonen, L. HSF1 at a glance. *J Cell Sci* **127**, 261–266 (2014).
36. Anckar, J. & Sistonen, L. Regulation of HSF1 Function in the Heat Stress Response: Implications in Aging and Disease. *Annu. Rev. Biochem.* **80**, 1089–1115 (2011).
37. Richter, K., Haslbeck, M. & Buchner, J. The Heat Shock Response: Life on the Verge of Death. *Mol. Cell* **40**, 253–266 (2010).
38. Wang, K. *et al.* Converting Redox Signaling to Apoptotic Activities by Stress-Responsive Regulators HSF1 and NRF2 in Fenretinide Treated Cancer Cells. *PLOS ONE* **4**, e7538 (2009).
39. Inouye, S. *et al.* Heat Shock Transcription Factor 1 Opens Chromatin Structure of Interleukin-6 Promoter to Facilitate Binding of an Activator or a Repressor. *J. Biol. Chem.* **282**, 33210–33217 (2007).
40. Walerych, D. *et al.* Hsp90 Chaperones Wild-type p53 Tumor Suppressor Protein. *J. Biol. Chem.* **279**, 48836–48845 (2004).
41. Kornmann, B., Schaad, O., Bujard, H., Takahashi, J. S. & Schibler, U. System-Driven and Oscillator-Dependent Circadian Transcription in Mice with a Conditionally Active Liver Clock. *PLOS Biol.* **5**, e34 (2007).
42. Miki, T., Matsumoto, T., Zhao, Z. & Lee, C. C. p53 regulates Period2 expression and the circadian clock. *Nat. Commun.* **4**, 1–11 (2013).
43. Zhang, R., Lahens, N. F., Ballance, H. I., Hughes, M. E. & Hogenesch, J. B. A circadian gene expression atlas in mammals: Implications for biology and medicine. *Proc. Natl. Acad. Sci.* **111**, 16219–16224 (2014).
44. Geyfman, M. *et al.* Brain and muscle Arnt-like protein-1 (BMAL1) controls circadian cell

proliferation and susceptibility to UVB-induced DNA damage in the epidermis. *Proc. Natl. Acad. Sci. U. S. A.* **109**, 11758–63 (2012).
45. Mullenders, J., Fabius, A. W. M., Madiredjo, M., Bernards, R. & Beijersbergen, R. L. A large scale shRNA barcode screen identifies the circadian clock component ARNTL as putative regulator of the p53 tumor suppressor pathway. *PLoS ONE* **4**, (2009).
46. Xiao, X. *et al.* HSF1 is required for extra-embryonic development, postnatal growth and protection during inflammatory responses in mice. *EMBO J.* **18**, 5943–5952 (1999).
47. Tsukada, T. *et al.* Enhanced proliferative potential in culture of cells from p53-deficient mice. *Oncogene* **8 12**, 3313–22 (1993).
48. Purvis, J. E. *et al.* p53 Dynamics Control Cell Fate. *Science* **336**, 13–16 (2012).
49. Schindelin, J. *et al.* Fiji: an open-source platform for biological-image analysis. *Nat. Methods* **9**, 676–682 (2012).
50. Tamaru, T. *et al.* CRY Drives Cyclic CK2-Mediated BMAL1 Phosphorylation to Control the Mammalian Circadian Clock. *PLoS Biol.* **13**, 1–25 (2015).
51. Bruning, O. *et al.* A range finding protocol to support design for transcriptomics experimentation: Examples of in-vitro and in-vivo murine UV exposure. *PLoS ONE* **9**, (2014).
52. Chen, H. & Boutros, P. C. VennDiagram: a package for the generation of highly-customizable Venn and Euler diagrams in R. *BMC Bioinformatics* **12**, 35 (2011).
53. Kutmon, M. *et al.* PathVisio 3: An Extendable Pathway Analysis Toolbox. *PLoS Comput. Biol.* **11**, 1–13 (2015).
54. van Iersel, M. P. *et al.* Presenting and exploring biological pathways with PathVisio. *BMC Bioinformatics* **9**, 399 (2008).
55. Kelder, T. *et al.* WikiPathways: Building research communities on biological pathways. *Nucleic Acids Res.* **40**, 1301–1307 (2012).
56. Kutmon, M. *et al.* WikiPathways: Capturing the full diversity of pathway knowledge. *Nucleic Acids Res.* **44**, D488–D494 (2016).
57. Xue, H., Slavov, D. & Wischmeyer, P. E. Glutamine-mediated dual regulation of heat shock transcription factor-1 activation and expression. *J. Biol. Chem.* **287**, 40400–40413 (2012).
58. Perry, M. E., Piette, J., Zawadzki, J. A., Harvey, D. & Levine, A. J. The mdm-2 gene is induced in response to UV light in a p53-dependent manner. *Proc. Natl. Acad. Sci. U. S. A.* **90**, 11623–7 (1993).
59. Li, D., Yallowitz, A., Ozog, L. & Marchenko, N. A gain-of-function mutant p53-HSF1 feed forward circuit governs adaptation of cancer cells to proteotoxic stress. *Cell Death Dis.* **5**, e1194 (2014).
60. Hirschie Johnson, C. 40 years of PRC. *Chronobiol. Int.* **16**, 711–743 (1999).
61. Engelen, E. *et al.* Mammalian TIMELESS Is Involved in Period Determination and DNA Damage-Dependent Phase Advancing of the Circadian Clock. *PLoS ONE* **8**, (2013).
62. Buhr, E. D., Yoo, S.-H. & Takahashi, J. S. Temperature as a Universal Resetting Cue for Mammalian Circadian Oscillators. *Science* **330**, 379–385 (2010).
63. Saini, C., Jorg, M., Stratmann, M., Gos, P. & Schibler, U. Simulated body temperature rhythms reveal the phase-shifting behavior and plasticity of mammalian circadian oscillators. *Genes Dev.* **26**, 567–580 (2012).
64. Jiang, W. *et al.* The circadian clock gene Bmal1 acts as a potential anti-oncogene in pancreatic cancer by activating the p53 tumor suppressor pathway. *Cancer Lett.* **371**, 314–325 (2016).
65. Oklejewicz, M. *et al.* Phase Resetting of the Mammalian Circadian Clock by DNA Damage. *Curr. Biol.* **18**, 286–291 (2008).
66. Gaddameedhi, S., Selby, C. P., Kaufmann, W. K., Smart, R. C. & Sancar, A. Control of skin cancer by the circadian rhythm. *Proc. Natl. Acad. Sci.* **108**, 18790–18795 (2011).

Chapter 3

本章については, 5 年以内に

雑誌等で刊行予定のため, 非公開.

Chapter 4

General Conclusions

In this dissertation, I aimed to prove the concept of combining the optical perturbation system and analysis of transcripts abundance for revealing the causative relationships in biological events. For this purpose, I described two topics, one is about the transcriptional architecture of circadian clock synchronization upon UV irradiation and the other is the integration of collective omics data upon specific perturbation of Akt activity using an optogenetic tool.

As a perturbation tool, optical stimulation was applied for both studies. However, the focus of the optical stimulation was different between the two studies. In circadian clock analysis, owing to the precise temporal stimulation by the optical perturbation system, temporal aspect of transcriptional regulation of clock gene *Per*2 during the circadian clock synchronization was the focus of the study. For the study of an integrative multi omics analysis of Akt, selective activation of Akt by the optical perturbation system, the PA-Akt system, to identify Akt responsible signaling network was highlighted. These studies demonstrate the advantages of applying optical perturbation system to reveal a mechanism of transcriptional regulation.

In **Chapter 2**, I utilized UV irradiation as an optical perturbation system and described an analytical framework to identify the causative regulation mechanism of *Per*2. For this research, I utilized the targeted approach of transcript quantification because the target is selected based on the previous literature.[1,2] The circadian clock is an oscillatory system and its phase of oscillation is a major factor characterizing circadian clock synchronization. In order to assess phases of the transcript expression, real-time monitoring of the transcript is necessary. Real-time monitoring of *Per2* expression was accomplished by monitoring temporal gene expression patterns using bioluminescent reporter assays upon different conditions. Temporal aspects of trans-activators involved in the circadian clock synchronization induced by UV exposure revealed that two stress-responsive transcription factors HSF1 and p53 cooperatively function to regulate expression of clock gene *Per*2 to reset the clock. Owing to a strong point of the reporter gene assay, I further succeeded in the characterization of circadian time-dependent aspects of HSF1 and p53 activation profiles, which suggested a strong relationship between the circadian system and stress-responsive pathways. I also demonstrated the use of unbiased approach, transcriptome analysis, for global assessment of transcriptional regulation upon optical stimulation by UV irradiation. The unbiased transcript measurement by microarray hybridization assay revealed that the HSR system activation and the circadian clock synchronization potentially regulates stress response pathways for cellular protection. Taken all in **Chapter 2**, I demonstrated the use of revealing temporal characteristics of transcription factors activation by bioluminescent reporters, which lead to the identification of molecular mechanism underlying synchronization of circadian clocks.

In **Chapter 3**, I described a method to integrate collective information from multiple molecular species to characterize causative relationships induced by specific Akt activation using the optogenetic system, the PA-Akt system. For this research, I used the unbiased approach for

transcripts quantification, since the effect of selective Akt activation on the transcripts were unknown. Omics analyses combined with optical perturbation by the PA-Akt system resulted in the identification of differentially regulated transcripts, metabolites, and phosphorylated proteins compared to insulin stimulation. Global assessment of the transcript revealed that Akt specific activation does not regulate transcripts as compared to insulin stimulation, however, the correlation of transcript changes was similar between the stimulations. Additionally, by comparing insulin-induced signaling network with that of Akt specifically induced signaling network from multi omics data including transcriptome, metabolome, and phosphorylated proteins, I succeeded in describing a signaling network that is sufficiently induced by selective Akt activation and also a signaling pathway that is not induced by Akt specific activation. Taken all in **Chapter 3**, a combination of molecule-specific perturbation by the optogenetic tool and global assessment of signaling molecules by omics analysis succeeded in the identification of novel signaling regulation modes.

Transcriptional regulation is a fundamental process in cellular systems. Transcriptional regulation research at first needs to identify responsible molecule for the regulation. This is usually performed with perturbation techniques. Conventionally, genetic methods are widely used for this purpose. Recently, with the advent of genome editing techniques, the genetic screening method of the responsible molecules using genome editing by the clustered regularly interspaced short palindromic repeats (CRISPR) system was developed. Because short guide RNA that the CRISPR system uses can be easily designed, a large-scale library of genetic variants using CRISPR genome editing can be constructed.[3] This method overcomes the weakness of conventional genetics in that generation time of genetic variants are shortened, which also results in avoiding cellular adaptation processes to occur. However, genetic techniques have a disadvantage in applying temporal perturbation, since the introduction of genetic mutations is a persistent process.

Another type of perturbation is a chemical perturbation. Because chemicals can either be an activator or an inhibitor of the target molecule, precise tuning of the perturbation can be achieved. Also, the administration pattern can be temporally controlled. The major concern of chemical perturbation is the specificity of the stimulation to the target molecule. Because some proteins especially isoforms share a common structure, specific binding to target molecule alone is difficult to achieve. Additionally, activating chemicals usually targets receptors on the plasma membrane. However, because the complex network of signaling occurs around the receptor, specific targeting of the signaling pathway activation by the receptor is difficult. As for Akt, the target molecule in **Chapter 3**, there is no known chemical to specifically activate it. These limitations highlight the difficulty in designing an experiment to use chemicals for revealing transcriptional regulation mechanisms for the target transcript.

Optical stimulation has the potential to overcome these issues. One of the advantages of optical stimulation is its temporal resolution of the stimulation, especially the off-time time resolution of the stimulation. Because the above-mentioned methods have longer off-time kinetics of the perturbation, the optical perturbation is most suited for the analysis of the biological system requiring perturbation at precise timings. In this dissertation, I used two types of optical stimulation, one is UV, which is environmental stress, and the other is an optogenetic tool. Since UV triggers activation of cellular adaptation systems for the perturbation, its use is limited to studies involving stress responses. However, UV irradiation has a unique property in that it stimulates endogenous signaling system of the cell with high temporal resolution. Because the circadian system can easily adapt to ectopic expression of a signaling molecule, introducing exogenous signaling system itself can perturb the circadian clock system. Thus, UV serves as a unique system that can perturb endogenous cellular system for the analysis of a temporal aspect of the circadian clock without modification of endogenous clock machinery. On the other hand, optogenetic tools target specific molecules for activation or inhibition. Because the introduction of optogenetic tools to cells are necessary, the optogenetic perturbation is not suited for a sensitive system like the circadian clock system. Despite that, activation of a specific molecule by optogenetic tools can be achieved in a high spatial and temporal manner. Hence, optogenetic tools are especially useful for perturbing specific molecule of interest.

In this dissertation, I described the analysis of causative relationships of transcriptional regulation using optical perturbation systems. Although candidate molecule or signaling responsible for the regulation can be estimated from the analyses of transcripts abundance, verification of the regulation modes requires additional information about signaling molecules. In **Chapter 2**, I utilized biochemical assays to show that candidate protein-protein interaction responsible for the regulation of the *Per2* transcription occurs UV simulation dependently. In contrast, in **Chapter 3**, I estimated the regulation modes by integrating information from global analysis data of the phosphorylated proteins. Both analyses succeeded in confirming the involvement of candidate signaling to the transcriptional regulation. However, they also indicate that combining verification methods are essential for the analysis of causative relationships. Further research would be needed to construct a framework to integrate efficient verification method for validating estimated molecule or pathway of regulation machinery.

In conclusion, I demonstratetintind that the combination of optical perturbation methods and transcript quantification methods pave the way to revealing causative relationships of biological events. Optical perturbation has two advantages. One is that optical stimulation can be delivered in high spatial and temporal resolution and the other is that specific actuation of the target molecule can be accomplished with optogenetic tools. Temporal analysis of transcript abundance after the optical perturbation is a powerful tool to analyze biological events which fluctuate over time, as shown in the

analysis of the circadian clock system. Molecule-specific activation by optogenetics is useful for analysis of the effect of a specific molecule, as shown with integrative multi omics analysis on Akt signaling. Both analyses contribute to the analysis of causative relationships in transcriptional regulation. One of the remaining topics in signaling network research is the identification of a feedback loop. Because signaling network consists of causative relationships of molecules, molecule-specific perturbation system is necessary. Moreover, feedback loop analysis requires analysis of molecule abundance change over time. Thus, further research would be to apply optical perturbation in molecule specific and in a temporal pattern manner simultaneously, which will contribute to the identification of feedback loops in the signaling pathways, leading to an understanding of precise network structure of signaling pathway consisting of a set of molecules.

References

1. Tamaru, T. *et al.* Synchronization of circadian Per2 rhythms and HSF1-BMAL1: clock interaction in mouse fibroblasts after Short-Term heat shock pulse. *PLoS ONE* **6**, 1–7 (2011).
2. Tamaru, T. *et al.* ROS stress resets circadian clocks to coordinate pro-survival signals. *PLoS ONE* **8**, 1–16 (2013).
3. Adamson, B. *et al.* A Multiplexed Single-Cell CRISPR Screening Platform Enables Systematic Dissection of the Unfolded Protein Response. *Cell* **167**, 1867-1882.e21 (2016).